Cell Communication and Signaling

RESEARCH

Open Access

BTN3A1 expressed in cervical cancer cells promotes Vγ9Vδ2 T cells exhaustion through upregulating transcription factors NR4A2/3 downstream of TCR signaling

Jian Liu[1,2], Min Wu[3], Yifan Yang[1], Xinyu Mei[1], Liming Wang[2], Jingyu Wang[1], Zixuan Wang[2], Shan He[2], Hangyu Liu[2], Han Jiang[2], Shen Qu[2], Yuwei Zhang[2], Ying Chen[1], Xun Tian[4*], Yafei Huang[5,6*] and Hui Wang[1,3,7,8*]

Abstract

Background Clinical trials have shown that immunotherapy based on Vγ9Vδ2 T cells (Vδ2 T cells) is safe and well-tolerated for various cancers including cervical cancer (CC), but its overall treatment efficacy remains limited. Therefore, exploring the mechanisms underlying the suboptimal efficacy of Vδ2 T cell-based cancer immunotherapy is crucial for enabling its successful clinical translation.

Methods Tumor samples from CC patients and CC cell line-derived xenograft (CDX) mice were analyzed using flow cytometry to examine the exhausted phenotype of tumor-infiltrating Vδ2 T cells. The interrelationship between BTN3A1 expression and Vδ2 T cells in CC, along with their correlation with patient prognosis, was analyzed using data from The Cancer Genome Atlas (TCGA) database. CC cell lines with BTN3A1 knockout (KO) and overexpression (OE) were constructed through lentivirus transduction, which were then co-cultured with expanded Vδ2 T cells, followed by detecting the function of Vδ2 T cells using flow cytometry. The pathways and transcription factors (TFs) related to BTN3A1-induced Vδ2 T cells exhaustion and the factors affecting BTN3A1 expression were identified by RNA-seq analysis, which was confirmed by flow cytometry, Western Blot, and gene manipulation.

Results Tumor-infiltrating Vδ2 T cells exhibited an exhausted phenotype in both CC patients and CDX mice. BTN3A1 expressed in CC is highly enhancing exhaustion markers, while reducing the secretion of effector molecules in Vδ2 T cells. Blocking TCR or knocking down nuclear receptor subfamily 4 group A (NR4A) 2/3 can reverse BTN3A1-induced exhaustion in Vδ2 T cells. On the other hand, IFN-γ secreted by Vδ2 T cells promoted the expression of BTN3A1 and PD-L1.

Conclusions Through binding γδ TCRs, BTN3A1 expressed on tumor cells, which is induced by IFN-γ, can promote Vδ2 T cells to upregulate the expression of TFs NR4A2/3, thereby affecting their activation and expression of exhaustion-related molecules in the tumor microenvironment (TME). Therefore, targeting BTN3A1 might overcome the immunosuppressive effect of the TME on Vδ2 T cells in CC.

Keywords BTN3A1, Cervical cancer, Tumor microenvironment, Adoptive T-cell therapy, Vγ9Vδ2 T cells, NR4A

*Correspondence:
Xun Tian
tianxun@zxhospital.com
Yafei Huang
huangy2018@hust.edu.cn
Hui Wang
huit71@sohu.com
Full list of author information is available at the end of the article

Introduction

Cervical cancer (CC) is a malignant tumor of the reproductive system that is caused mainly by HPV infection. Every year, more than 500,000 women worldwide are diagnosed with CC, resulting in 300,000 deaths [1]. Unfortunately, the prognosis for women with metastatic or recurrent cancer remains unfavorable, despite the use of novel immune checkpoint inhibitors (ICIs) [2, 3]. Therefore, it is crucial to explore effective and innovative treatment strategies to improve the outlook for CC patients.

Recent study has shown that γδ T cells are strongly associated with a favorable prognosis in patients with benign tumors across 39 different types of cancers and approximately 18,000 samples [2]. Notably, γδ T cells have demonstrated potent anti-tumor effects on various types of cancer cells, independent of the major histocompatibility complex (MHC) restriction [4]. As a result, there is a renewed interest in utilizing γδ T cells for cancer immunotherapy, including CC [5, 6]. Currently, the most commonly used subset of γδ T cells for immunotherapy is the Vδ2 T cell subset. These cells can be manipulated through in vivo stimulation with amino-bisphosphonates or through adoptive cell transfer therapy after in vitro activation and expansion with amino-bisphosphonates or synthetic phosphorantigens (pAgs).

Despite the potential of Vδ2 T cell-based immunotherapy as a promising therapeutic strategy for cancers, its overall efficacy remains relatively low in several cancer types [6]. This limited efficacy is likely attributable to the poor infiltration of adoptively transferred Vδ2 T cells and the influence of the immunosuppressive TME. Indeed, functional impairment of γδ T cells has been observed in terminal cancer patients with B cell tumors [7]. Additional studies have demonstrated that γδ T cells exhibit reduced infiltration and frequently undergo immune tolerance and exhaustion within the TME of various solid tumors [8–10]. The underlying mechanisms contributing to the exhaustion or dysfunction of γδ T cells warrant further investigation [11].

Studies on αβ T cells have demonstrated that the primary cause of T cells exhaustion is prolonged antigenic stimulation of TCR, which triggers the phosphorylation of the kinases Lck and ZAP70. This activation triggers a cascade of pathways that regulates TFs and genes related to the effector or exhaustion functions of T cells [12, 13]. Among these TFs, members of the NR4A family have garnered particular attention due to their stable expression in tolerant $CD8^+$ T cells. In addition, elevated levels of NR4A TFs have been observed in T cells from individuals with cancer or chronic viral infections [14]. Notably, NR4A TFs are overexpressed in exhausted T cells, which is associated with increased expression of PD-1 and TIM3, and diminished cytotoxicity [15]. Therefore, NR4A TFs are the main participants in T cell exhaustion. However, it is uncertain if Vδ2 T cell exhaustion follows the same mechanism, requiring further study.

BTN3A1, a B7 immunoglobulin superfamily member widely expressed on immune cells including antigen presentation cells (APCs), is an important TCR ligand for pAg-induced Vδ2 T cell activation [16, 17]. Interestingly, BTN3A1 is highly expressed in many cancers and is linked to clinical outcomes of 13 types of cancer [18]. B7 family proteins, known for their immune regulatory roles, are targets for immune checkpoint therapy [19, 20]. It is speculated that chronic BTN3A1 binding with γδ TCRs in the TME may cause γδ T cell dysfunction [21], although this is unconfirmed.

To address these challenges, our study clarified the exhaustion of tumor-infiltrating Vδ2 T cells in CC, and investigated how BTN3A1 expression in CC cells induces this exhaustion. We found that Vδ2 T cells in CC tissue show higher levels of exhaustion markers (e.g., PD-1, TIM3, and LAG3) compared to those in peripheral blood mononuclear cells (PBMCs). BTN3A1 expressed in CC cells can promote the exhaustion of in vitro–amplified Vδ2 T cells by impacting the TCR and NF-κB signaling pathways and regulating the expression of TFs, including NR4A2/3, TOX, and EOMES, and exhaustion markers. In turn, the IFN-γ secreted by activated Vδ2 T cells boots the expression of PD-L1 and BTN3A1 in tumor cells and immune cells, thereby increasing the immunosuppressive capacity of TME. Therefore, BTN3A1 may serve as a novel immune checkpoint molecule that could potentially synergize with anti-PD-1/PD-L1 antibodies.

Materials and methods

Human samples

This study was approved by the Medical Ethics Committee of Tongji Medical College, Huazhong University of Science and Technology (Approval No. [2021] S034). A total of 20 patients with CC were included in this study (20 samples of peripheral blood and 13 specimens of tumor tissue were collected). The patient demographics is presented in Table S1. In addition, peripheral blood samples were collected from healthy adult donors. All the required samples were obtained after signing a written informed consent form from the participants. A density gradient centrifugation method based on Ficoll-Paque was used to separate PBMCs of healthy donors and CC patients, and the obtained PBMCs were used for flow cytometry detection and expansion of Vδ2 T cells in vitro.

Preparation of tissue single-cell suspension

Using ophthalmic scissors cut the tumor tissue specimen into approximately 1 mm^3 pieces and place them into C tubes. Add digestive solution (collagenase I + collagenase IV + EDTA (Ethylene diamine teraacetic acid) solution + HBSS) and shake with a tissue disintegrator (Miltenyi Biotec) for 30 s, then incubate on a shaker at 37 °C for 30 min. Add complete culture medium to terminate digestion, filter out cell clumps using a 70 μm sterile cell filter, centrifuge at 1500 rpm for 5 min. Add red blood cell lysis buffer to the cell precipitate for 3–5 min, wash with sterile PBS, centrifuge at 1500 rpm for 5 min. Resuspend the cell precipitate in cell cryopreservation protective solution, and freeze it in liquid nitrogen for subsequent experiments. The cell viability is (mean ± SD) 67.09 ± 20.64%.

Tumor cell lines and cell culture

Cervical cancer cell lines (SiHa, HeLa-luci, CasKi, C33A, MS751) were cultured in RPMI DMEM medium with 10% fetal bovine serum (FBS) added (12800–58, Gibco, Life Technologies). The CC cell line ME-180 was cultured in improved McCoy's 5a medium with 10% FBS added.

Construction of animal models

NCG (NOD/ShiLtJGpt-Prkdcem26Cd52Il2rgem26Cd22/Gpt), female mice, 6–8 weeks old, were purchased from GemPharmatech (Nanjing, China). All mice were raised in the isolation system of the SPF Animal Laboratory at the Experimental Animal Center of Tongji Hospital affiliated to Huazhong University of Science and Technology. This study was approved by the Experimental Animal Ethics Committee of Tongji Hospital Affiliated to Huazhong University of Science and Technology (Approval No. [2022] IACUC Number:3830).

The CDX tumor model was established using 6–8-week-old female NCG mice. HeLa-luci cells (2×10^6) and CaSki cells (1×10^7) were resuspended in 100 μl of culture medium and were subcutaneously inoculated into NCG mice with insulin needles. When the tumor grew to the size of a soybean and could be palpated (50 mm^3), the tumor-bearing mice were randomly allocated into different groups to ensure that the tumor load of each group of mice was similar. After grouping, expanded Vγ9Vδ2 T cells (1×10^7 cells per mouse) were transferred via the tail vein into tumor-bearing mice. Tumor tissues were collected and digested into single-cell suspension for flow cytometry after adoptive transfer. The growth of tumors was continuously monitored and the survival of mice was recorded as indicated. Mice with tumors greater than 2000 mm^3 in size are considered to have reached the endpoint of life and are marked as dead in survival records.

In vitro culture and amplification of Vδ2 T cells

PBMCs were seeded at a density of 2×10^6 cells per well in the 6-well plates, and cultivated in X-vivo medium with 10% FBS added (04-418Q, LONZA). At the beginning of amplification (day 0), zoledronic acid salt (Sigma) (5 μM) and recombinant human IL-2 (1000 IU/ml) were added to the culture medium. After 4 days, the culture system was replaced with fresh culture medium also containing 5 μM zoledronic acid salt and 1000 IU/ml IL-2. In the subsequent culture, cells were counted daily and fresh culture medium containing 1000 IU/ml IL-2 was added to maintain cell density within the range of $0.8–1.2\times10^6$/ml. On the 12th day of cultivation, a certain number of cultured cells were cultured with tumor cells followed by detecting the characteristics of Vδ2 T cells including exhaustion, activation, killing, and anti-tumor potential.

siRNA and lentiviral transduction

The siRNAs targeting NR4A2/3 were designed and synthesized by General Biol (Anhui, China). Lipofectamine 3000 (Life Technologies) was used to deliver the siRNAs to Vδ2 T cells, and the most effective siRNA was then screened for subsequent functional research. BTN3A1 plasmid packaged with lentivirus was purchased from Yunzhou Biotechnology (Guangzhou, China). The CaSki-BTN3A1-OE cell lines were established by stably transducing with a lentivirus vector encoding the hBTN3A1[NM_007048.6]-EGFP. The Hela-BTN3A1-KO cell lines were established by stably transducing with hCas9-hBTN3A1[gRNA#839]-EGFP. The HPV-E7 gene overexpression lentivirus was purchased from GeneRulor Biotechnology (Zhuhai, China) and was transfected into indicated tumor cells. 24 h after transfection, tumor cells were screened with 2 μg/ml puromycin (Selleck). The surviving tumors were amplified and used for subsequent experiments.

Detection of cell proliferation

For the Cell Counting Kit-8 (CCK-8) assay, tumor cells were seeded onto a 96-well plate at a density of 3,000 cells per well, and cell proliferation was evaluated using CCK8 Cell Counting Kit (A311, Vazyme). For the colony-formation assay, a total of 250 or 500 cells were seeded in a six-well plate and cultured in DMEM containing 10% FBS for 2 weeks. The clones were fixed in 4% paraformaldehyde and stained with crystal violet before being photographed. For Cell Trace violet (CTV) proliferation detection, a certain amount of Vδ2 T cells was collected and resuspended with PBS, Cell Trace Violet Cell Proliferation Kit (C34557, Invitrogen) was subsequently used for CTV staining, followed by co-culturing with tumor cells to detect the dilution level of CTV by flow cytometry.

Flow cytometry

The antibodies used for flow cytometry detection in Table S2. Antibodies against human antigens used for flow cytometry were listed as target antigen. Single-cell suspensions were prepared from tumor tissues, peripheral blood or co-cultured cells, and a pipette was used to transfer indicated number of cells in 100 μl of medium into a flow cytometry tube, and make the total number of cells equal in each flow cytometry tube through cell counting (the number of cells added to the flow cytometry tube may vary in different experiments and staining panels). Each tube was replenished with 3 ml of flow cytometry staining buffer, and centrifuged at 4 °C and 1500 rpm for 5 min. Subsequently, the supernatant was discarded and cells were incubated with reactive dyes FVS (BD) followed by Fc block (B313423, Biolegend) for 15 min each. Staining for surface markers were performed by mixing cells with fluorescein-labeled antibodies and incubation at 4 °C for 30 min. For intracellular staining, cells were treated with Cytofix/Cytoperm Fixation/Permeabilization Kit (554714, BD) for fixation and breaking cell membrane after surface protein staining. For intracellular staining of cytokines, cells were incubated with the addition of PMA, ionomycin and brefeldin A (423303, Bioledgend) for 5 h before proceeding to intracellular staining. For intranuclear staining, cells stained with fluorescein-labeled antibodies against surface proteins were fixed and permeabilized using a Transcription Factor Buffer Set (562574, BD), followed by staining intracellular proteins with mixed antibodies labeled with fluorescein.

Flow cytometry analysis was performed using LSR Fortessa Cytometer (BD) and The ID7000™ spectral cell analyzer, with 10,000 targeted events acquired. When analyzing the flow cytometry data, all cells were gated based on forward (FSC-A) and lateral (SSC-A) scattering, and then single cells were gated using FSC-A and FSC-W parameters to exclude debris, followed by gating live cells by FVS staining. The tumor infiltrating Vδ2 T cells were identified as $CD3^+V\delta2^+$. Peripheral circulating and in vitro expanded Vδ2 T cells were identified as $CD3^+V\delta2^+$ or $CD3^+\gamma\delta$ TCR^+. Tumor cells in the co-culture system were identified as $CD3^-V\delta2^-$. The exhaustion, activation and killing potential of Vγ9Vδ2 T cells were determined by the expression of surface proteins PD-1, TIM3, LAG3, HLA DR, CD86, NKG2D, FasL, PD-L1, intracellular expression of IFN-γ, TNF-α, PRF1, IL-17A and GZMB, as well as the expression of TOX, NR4A1, NR4A2, and NR4A3 in the nucleus.

To detect the killing effect of Vδ2 T cells on tumor cells after co-culture, Annexin V-PE/7-AAD apoptosis detection kit (559763, BD) was used to stain the cell and detect the apoptosis of tumor cells. When analyzing the flow cytometry data, all cells were gated based on FSC-A and SSC-A scattering, and then tumor cells in the co-culture system were identified as $EGFP^+$ and $CD3^-V\delta2^-$. The dead tumor cells were identified as Annexin V-PE^+7-AAD^+. To test the antigen-processing ability of Vδ2 T cells, DQ-OVA (D12053, Invitrogen) was added to the co-culture system of Vδ2 T cells and tumor cells, and the ability of Vδ2 T cells to phagocytose DQ-OVA was detected by flow cytometry.

Immunohistochemistry

Paraffin sections of tumor tissue and adjacent tissue from CC patients were placed in an electric thermostatic drying oven at 65 °C for 2 h for dewaxing and hydration. Sections were then placed in antigen repair solution and heated at a high temperature in a microwave oven. After natural cooling, the sections were treated with 3% H_2O_2 at 37 °C for 15 min to block the endogenous peroxidase activity. Subsequently, non-specific antigens were blocked by incubation with 5% bovine serum albumin (BSA) at 37 °C for 30 min. The sections were incubated with anti-BTN3A1 Ab (PA5-97513, Invitrogen) at 1:100 in a refrigerator overnight at 4 °C. After washing, the secondary antibody was added dropwise and incubated at 37 °C for 30 min. Subsequently, DAB staining was performed and nuclei was stained with hematoxylin. Finally, the sections were dehydrated and the slides were sealed for observation under a microscope.

Western blot (WB)

RIPA Lysis Buffer (G2002, Servicebio, China) was used to lyse proteins in cells and the proteins were transferred them onto PVDF membranes via wet transfer, followed by sealing in 5% skim milk powder for 1 h. Membranes were incubated with specific primary antibody overnight at 4 °C. The antibodies used for WB detection in Table S2. Membranes were then incubated with the secondary antibody in a constant temperature shaker for 1 h, followed by revealing the protein expression level using Western Bright ECL HRP substrate (K-12045-D50, Advansta) and chemiluminescence imaging system (Bio-Rad).

Quantitative real-time polymerase chain reaction (qRT–PCR)

Total RNA was extracted from cultured cells using RNA extraction kit (RC112, Vazyme), and then reverse transcribed into cDNA using reverse transcription kit (R223, Vazyme). Perform RT-PCR using a ChamQ Universal SYBR qPCR Master Mix (Q711, Vazyme) and MiniOpticon RT-PCR system (Bio-Rad). The primers were used for qRT-PCR in Table S3.

Enzyme linked immunosorbent assay (ELISA)

The supernatant was collected from the co-culture system containing tumor cells and Vδ2 T cells, and an IFN-γ ELISA Kit (430104, Biolegend) was used to detect the secretion of IFN-γ by Vδ2 T cells at different time points after co-culturing.

Detection of BTN3A1 expression level on membrane surface of cells

To detect the expression level of BTN3A1 on the surface of CC cell lines, SiHa, HeLa-luci, CaSki, C-33A, MS751, ME-180 were stained with BTN3A1 mAb (eBioBT3.1, Invitrogen) or homotypic control (14–4714, Invitrogen) at 4 °C for 30 min, and the cells were detected by flow cytometry. To detect the expression level of BTN3A1 on the membrane surface of CC cells stimulated by IFN-γ, CC cell lines (CaSki and HeLa-luci) were treated with IFN-γ (100 ng/ml, 570202, Biolegend), co-cultured with or without the addition of anti-human IFN-γ neutralizing antibody (10 ng/ml, 506531, Bioledgend) for 24 h, and cells were collected for detection using flow cytometry. To detect whether Vδ2 T cells can induce BTN3A1 expression in CC cells by secreting IFN-γ, HeLa-luci cells and Vδ2 T cells were co-cultured with or without the addition of anti-human IFN-γ neutralizing antibodies for 24 h, and flow cytometry were used to detect the expression level of BTN3A1 on the surface of tumor cells.

Bioinformatics analysis

RNA-seq data for the STAR process of the TCGA-CESC (cervical squamous cell carcinoma and adenocarcinoma) project were downloaded and organized from the TCGA database (https://portal.gdc.cancer.gov/), and FPKM format data as well as clinical data were extracted. The Xiantao tool platform was utilized (https://www.xiantao.love/) to analyze correlations between molecules. BEST database was applied (https://rookieutopia.com/app_direct/BEST/) to analyze the survival prognosis of tumor patients and the impact of BTN3A1 expression on immunotherapy. The TIMER 2.0 database (http://timer.cistrome.org/) was applied to analyze the correlation between γδ T cell infiltration levels and the prognosis of CC patients, as well as the impact of BTN3A1, NR4A2/3 and γδ T cells on the survival prognosis of patients.

RNA sequencing and analysis

After co-culturing Vδ2 T cells with tumor cells, Vδ2 T cells were sorted using human TCRγ/δ^+ T Cell Isolation Kit (Miltenyi Biotec), according to the manufacturer's instructions and total RNA was extracted. An mRNA library was established using Illumina technology platform. RNA sequencing was performed on BGI-SEQ platform with the running of quality control. The analysis of sequencing data, including gene heatmaps, was conducted by BGI Gene Dr Tom analysis platform.

Statistical analysis

The flow cytometry data were analyzed and plotted using Flow Jo 10.4 software, and the data were analyzed and plotted using Prism 8.3 (Graphpad software). The data in the figure are presented in terms of mean ± standard deviation (SD). The statistical test adopts a two-tailed Student's *t*-test. $p < 0.05$ is considered statistically significant, and statistical differences are represented by asterisks: ****/####$p < 0.0001$, ***/###$p < 0.001$, **/##$p < 0.01$, */#$p < 0.05$.

Results

Tumor cells promote the expression of exhaustion-related molecules in Vδ2 T cells

Exhausted γδ T cells have been identified in the TME of various cancers, including neuroblastoma, pancreatic ductal adenocarcinoma, colorectal cancer, multiple myeloma (MM), and kidney cancer [22]. To investigate if Vδ2 T cells in CC also exhibit an exhaustion phenotype, we compared the expression of exhaustion markers (e.g., PD-1, TIM3, and LAG3) in Vδ2 T cells from the peripheral blood and tumor tissue of CC patients (Fig. 1A). Results indicated that higher levels of PD-1 and TIM3, especially PD-1, in tumor-derived Vδ2 T cells compared to those from peripheral blood.

We subsequently aimed to explore the functional changes of Vδ2 T cells following their infiltration into the TME. Upon subcutaneously implanted HeLa-luci cells in NCG mice grew to palpable tumor (day 12 after injection), Vδ2 T cells expanded for 12 days adoptively transferred via tail vein into CDX-bearing mice (Figure S1A). The expression levels of activation and exhaustion-related molecules on the tumor-infiltrating Vδ2 T cells

(See figure on next page.)

Fig. 1 Upregulated expression of exhaustion-related molecules in Vδ2 TILs from CC. **A** Percentages of PD-1$^+$, TIM3$^+$ and LAG3$^+$ cells (left and upper right), and the expression levels (MFIs) of PD-1, TIM3 and LAG3 (lower right) in Vδ2 T cells from peripheral blood ($n = 20$) and tumor tissue ($n = 13$) of CC patients. **B** An animal experimental system for in vivo evaluation of the impact of CC cells on adoptively transferred Vδ2 T cells. **C** MFIs of IFN-γ, TNF-α, PD-1, and TOX proteins in Vδ2 TILs on day 0 (D12), day 4 (D16), day 6 (D18), and day 8 (D20) after adoptive transfer ($n = 4$ mice per group). **D** Percentages of PRF1$^+$ (upper panel), IFN-γ$^+$TNF-α$^+$ (middle panel), and PD-1$^+$TOX$^+$ cells (lower panel) Vδ2 T cells ($n = 3$ healthy donors) after Vδ2 T cells cultured alone or co-cultured with CC cell line HeLa-luci for 6 h or 24 h. Error bars represent mean ± SD. *P* values were calculated using two-tailed Student's *t* test. ****/####$p < 0.0001$, ***$p < 0.001$, **$p < 0.01$, */#$p < 0.05$. ns, not significant. MFI, mean fluorescent intensity

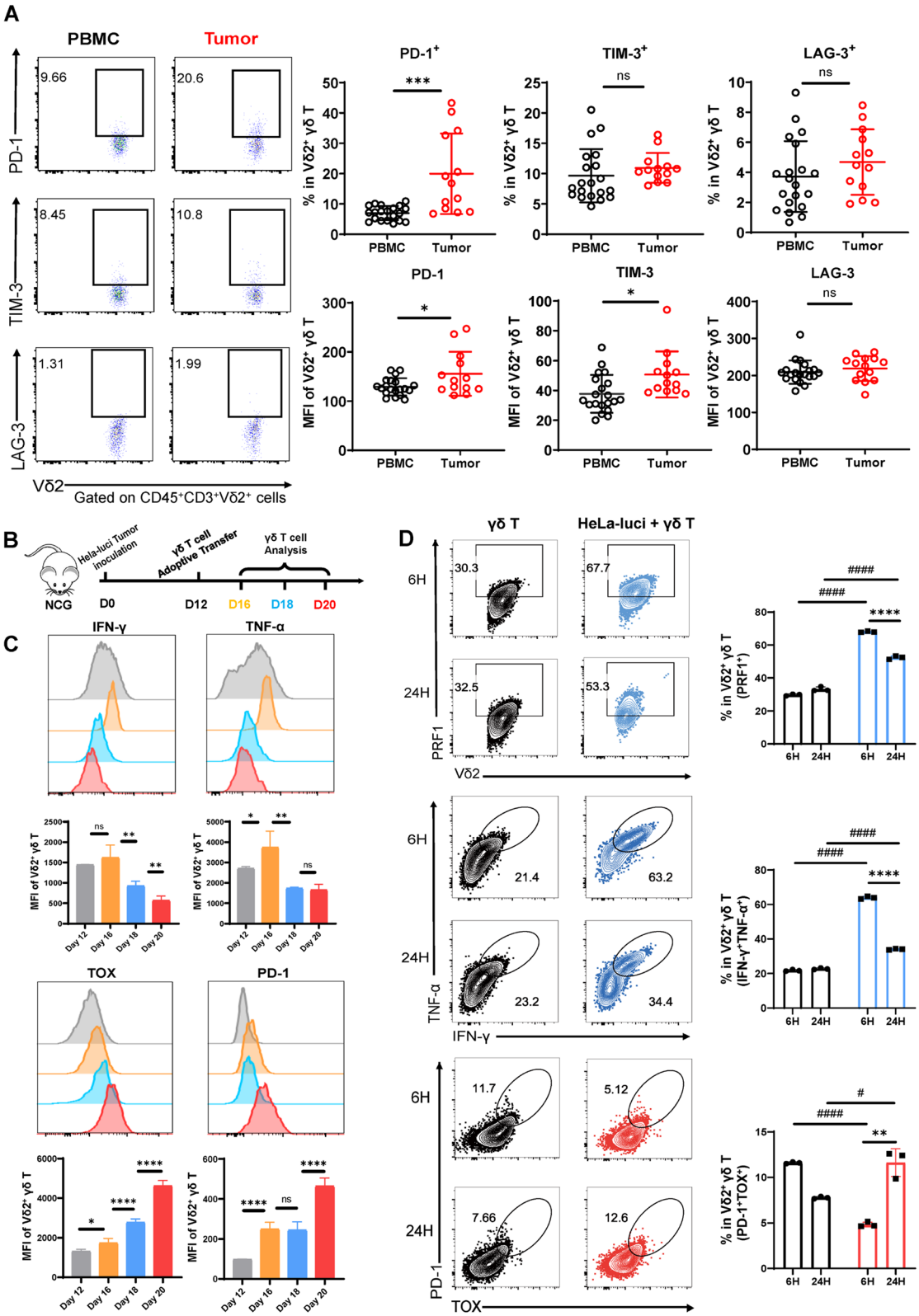

Fig. 1 (See legend on previous page.)

were determined on the 4th, 6th, and 8th day after adoptive transfer (Fig. 1B). After adoptive transfer, tumor-infiltrating Vδ2 T cells showed increased IFN-γ and TNF-α secretion by day 4, which then gradually decline. Concurrently, the exhaustion markers PD-1 and TOX gradually upregulated [23] (Fig. 1C), suggesting that Vδ2 T cells might rapidly enter the exhaustion program under the influence of TME.

To determine the direct impact of CC cells on the functionality of Vδ2 T cells, the expanded Vδ2 T cells were co-cultured with HeLa-luci cells in vitro. Post co-culture, levels of cytotoxicity molecules PRF1, IFN-γ, and TNF-α in Vδ2 T cells significantly increased after 6 h of co-culture, while the percentage of PD-1^{+}TOX^{+} Vδ2 T cells is decreased, indicating that tumor cell-induced activation of Vδ2 T cells. However, upon extending the co-culture duration to 24 h, the expression levels of cytotoxicity-related molecules on Vδ2 T cells were significantly decreased, and the percentage of PD-1^{+}TOX^{+} Vδ2 T cells was markedly higher than those co-cultured for 6 h and those cultured alone (Fig. 1D). Therefore, these results demonstrate that CC cells within the TME directly induce the activation and promote the exhaustion of Vδ2 T cells.

BTN3A1 and γδ T cells affect the prognosis of CC patients

BTN3A1 is a crucial ligand for TCR Vγ9Vδ2, which plays an indispensable role in pAgs-induced Vδ2 T cell activation when expressed in APCs and/or tumor cells [16]. Indeed, during the process of Vδ2 T cell expansion in vitro, the expression levels of BTN3A1 increased on CD3^{-} non-T cells, CD3^{+}Vδ2^{-} and Vδ2^{+} T cells in the initial days, which is consistent with the proliferation curve of Vδ2 T cells, highlighting the key role of BTN3A1 in Vδ2 T cells proliferation and early activation (Fig. 2A and Figure S1A). In addition, KEGG and GO analysis of the CC data from TCGA database showed that BTN3A1 mainly influences immune-related pathways, including antigen presentation and TCR signaling, thereby underscoring its important role in the immune regulation of CC (Figure. S1B and S1C). Conversely, RNA-seq analysis of clinical samples revealed that the expression level of BTN3A1 in CC tissue was markedly elevated than that in adjacent cervical tissue (Fig. 2B). In line with this result, immunohistochemistry also revealed that the expression level of BTN3A1 in CC tissue was higher than that in adjacent tissues, and it was mostly expressed in cancer nests (Fig. 2C). Importantly, low BTN3A1 expression was positively correlated with overall survival (OS) ($p=0.022$), progression-free survival (PFS) ($p=0.035$), and disease-free survival (DFS) in the GSEA ($p=0.036$) and TCGA ($p=0.024$) databases (Fig. 2D and Figure S1D). Thus, these results collectively suggest that BTN3A1 has a pro-tumoral role in CC.

The correlation between BTN3A1 expression and γδ T cells infiltration with patient prognosis was analyzed. Interestingly, patients exhibiting low expression of BTN3A1 coupled with high γδ T cell infiltration had the highest survival rate, whereas those with high BTN3A1 expression and low γδ T cell infiltration had the lowest survival rate. Moreover, although the frequency of γδ T cells was significantly associated with patient survival rates, the difference disappeared in patients with high BTN3A1 expression (Fig. 2E and Figure S1E). At the same time, BTN3A1 expression is positively correlated with exhausted molecules (e.g., *PDCD1, HAVCR2, LAG3* and *TOX*) (Fig. 2F). Together, these results suggest that the pro-tumoral effect of BTN3A1 may be mediated via γδ T cells.

BTN3A1 expressed by tumor cells promotes Vδ2 T cells exhaustion

Although antigen stimulation is required for the activation of αβ T cells, it induces αβ T cell exhaustion when presents persistently. We hypothesized that BTN3A1 expression by CC cells might similarly contribute to Vδ2 T cell exhaustion. To test this speculation, we constructed BTN3A1-KO and -OE CC cell lines, based on the varying expression levels of BTN3A1 across different CC cell

(See figure on next page.)

Fig. 2 BTN3A1 and γδ T cells affect patient prognosis. **A** MFI of BTN3A1 in Vδ2^{+} cells, CD3^{+} cells, and CD3^{-} cells ($n=3$ healthy donors) during the expansion of Vδ2 T cells in vitro using PBMCs from healthy individuals. **B** mRNA expression levels of *BTN3A1* in normal ($n=32$) and tumor tissue ($n=127$) of CC patients. **C** Representative images of BTN3A1 expression in tumor and adjacent tissues of CC patients. Scale bar: 200 μM. **D** The correlation between the mRNA expression level of *BTN3A1* and overall survival (OS) as well as progression free survival (PFS) in CC patients ($n=299$) in the TCGA dataset. **E** The correlation between the combination of mRNA expression level of *BTN3A1* and infiltration level of γδ T cells, and the cumulative survival rate of CC patients in the TCGA database ($n=306$), analyzed using TIMER 2.0. **F** The correlation between the mRNA expression level of *BTN3A1,* and that of genes related to exhaustion in CC patients in the TCGA database ($n=306$). **G** Detection of protein expression of BTN3A1 in cervical cancer cell lines (upper panel), and validation of the constructed cell lines with BTN3A1 overexpression and knockout (lower panel). **H** The number of clones formed (counting clones > 50 cells) after 250 and 500 CaSki cells and HeLa-luci cells were plated onto a six well plate ($n=3$ replicates per group). **I**, **J** Tumor growth curves (**I**) and survival proportions of (**J**) tumor-bearing NCG mice implanted with CaSki (BTN3A1-WT or BTN3A1-OE) cell lines subcutaneously ($n=10$ per mice group). Error bars represent mean ± SD. *p* values were calculated using two-tailed Student's *t* test. Survival curves were calculated with Log-rank (Mantel–Cox) test. ****$p<0.0001$. ns, not significant

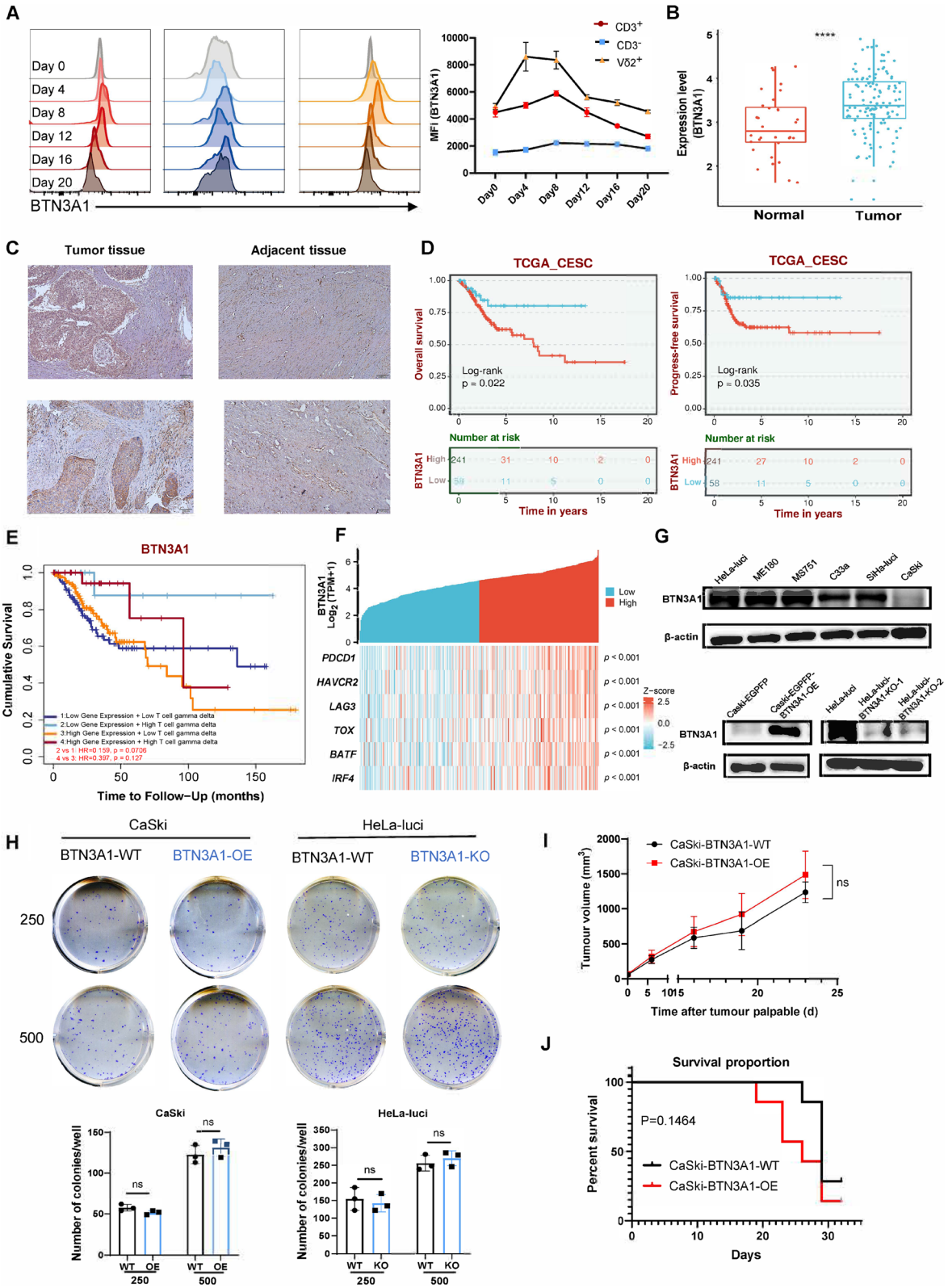

Fig. 2 (See legend on previous page.)

lines (Fig. 2G and Figure S2A). In vitro colony-forming and CCK-8 assays demonstrated that manipulation of BTN3A1 expression did not affect the proliferation of CC cells (Fig. 2H and Figure S2B). Furthermore, when BTN3A1-WT and BTN3A1-OE cell lines were subcutaneously implanted into NCG mice, they had no effect on tumor proliferation and mice survival (Fig. 2I and J). Therefore, BTN3A1 does not seem to have an intrinsic effect on CC cells.

Given that HPV is the main inducing factor of CC, we need to investigate the influence of HPV16 and HPV18 E6 and E7 oncoproteins on the expression of BTN3A1, as well as their potential impact on the functionality of Vδ2 T cells as cancer antigens. The results indicated that while CaSki cells exhibited high levels of E6 and E7 expression, BTN3A1 expression was notably low (Figure S2C). Furthermore, overexpression of the E7 protein in C33A cell lines, which are negative for both HPV16 and HPV18, did not result in increased expression of BTN3A1 (Figure S2D). Therefore, no significant correlation was observed between the expression levels of E6 and E7 and the expression of BTN3A1. At the same time, the ability of Vδ2 T cells to secrete IL-17A in response to various CC cell lines did not exhibit a correlation with the expression levels of the HPV E6 and E7 proteins (Figure S2E).

To assess the impact of BTN3A1 on Vδ2 T cells in CC cells, we co-cultured Vδ2 T cells with CC cell lines varying in BTN3A1 expression for 24 h and then sorted them for RNA-seq. Compared to the WT group, the expression levels of exhaustion-related molecules (*PDCD1*, *HAVCR2*, *LAG3*, *TOX*, etc.) of Vδ2 T cells were significantly upregulated in the BTN3A1-OE group and downregulated in the BTN3A1-KO group (Fig. 3A). Furthermore, the expression of Vδ2 T cells exhaustion-related molecules in the co-culture system was detected, finding that the expression of PD-1, TIM3, and LAG3 in the BTN3A1-KO group was lower than that in the WT group, while the expression in the BTN3A1-OE group was higher than that in the WT group (Fig. 3B, Figure S3A and S3B). Moreover, the percentage of PD-1^{+}TIM3^{+} Vδ2 T cells was also significantly reduced in the BTN3A1-KO group (Figure S3C). Next, Vδ2 T cells were co-cultured with irradiated tumor cells to exclude the influence of other factors (such as tumor supernatant). PD-1, TIM3, and LAG3 expression in Vδ2 T cells remained lower in the BTN3A1-KO group than in the WT group (Fig. 3C). Meanwhile, compared to those in the WT group, Vδ2 T cells in the BTN3A1-KO group exhibited enhanced secretion of IFN-γ and TNF-α (Fig. 3D and Figure S3D), higher expression of perforin (PRF1) and granzyme B (GZMB) (Fig. 3E), as well as stronger proliferating ability (Figure S3F). In contrast, Vδ2 T cells from the BTN3A1-OE group were relatively weaker (Figure S3E and S3G).

In order to detect the anti-tumor capability of Vδ2 T cells after co-culturing, Vδ2 T cells were sorted out and further co-cultured with tumor cells for 6 h. Apoptosis detection revealed that Vδ2 T cells in the BTN3A1-KO group had a stronger tumor-killing ability, whereas those in the BTN3A1-OE group had a weaker ability compared to the BTN3A1-WT group (Fig. 3F). Previous studies have shown that Vδ2 T cells have strong antigen presentation ability, which can further promote anti-tumor ability of CD8^{+} T cells [4], we thus explored the expression levels of antigen presentation-related molecules on Vδ2 T cells after co-culturing with tumor cells. The expression levels of HLA-DR and CD86 in Vδ2 T cells reached over 90%, with no significant difference observed between the two groups at 48 h (Figure S4A and S4B). But after co-culturing, Vδ2 T cells in the BTN3A1-KO group exhibited a higher average mean fluorescence intensity (MFI) of DQ-OVA, indicating that they had stronger antigen processing ability than those in the BTN3A1-WT group (Fig. 3G). Taken together, these findings indicate that high expression of BTN3A1 in CC cells induces exhaustion or functional impairment in Vδ2 T cells in vitro.

Additionally, through single T cell analysis by RNA-seq and TCR tracking (STARTRAC) analysis, Zhang L et al.

(See figure on next page.)

Fig. 3 BTN3A1 promotes Vδ2 T cells exhaustion. **A** Heatmap showing log2FC fold changes for the differentially expressed genes of selected exhaustion-related molecules of Vδ2 T cells co-cultured with CaSki (BTN3A1-OE *vs.* BTN3A1-WT, left) and HeLa-luci (BTN3A1-KO *vs.* BTN3A1-WT, right) tumor cell lines at a 1:1 ratio for 24 h ($n=2$ replicates per group). **B** Percentages of PD-1^{+}, TIM3^{+}, and LAG3^{+} cells in Vδ2 T cells after co-culturing Vδ2 T cells with HeLa-luci (BTN3A1-WT and BTN3A1-KO) tumor cell lines at a 1:1 ratio for 24 h. **C** Percentages of PD-1^{+}, TIM3^{+}, and LAG3^{+} cells in Vδ2 T cells after co-culturing with irradiated (50 Gy) HeLa-luci (BTN3A1-WT and BTN3A1-KO) tumor cell lines at a 1:1 ratio for 24 h. **D**, **E** Vδ2 T cells cultured with HeLa-luci (BTN3A1-WT and BTN3A1-KO) tumor cell line at a 1:1 ratio for 24 h, percentage of IFN-γ^{+}TNF-α^{+} cells and MFIs of IFN-γ, TNF-α in Vδ2 T cells (**D**); percentage of PRF1^{+}GZMB^{+} cells and MFIs of PRF1, GZMB in Vδ2 T cells (**E**) ($n=3$ healthy donors). **F**, **G** Vδ2 T cells were sorted out after co-culturing with HeLa-luci (BTN3A1-WT and BTN3A1-KO) and CaSki (BTN3A1-WT and BTN3A1-OE) cell lines, and then co-cultured with BTN3A1-WT tumor cells at a 1:1 ratio for 6 h. Percentage of Annexin V^{+}7-ADD^{+} cells in tumor cells ($n=3$ healthy donors) (**F**); Percentage of Vδ2 T cells phagocytosing DQ-OVA after 6 h of addition ($n=4$ healthy donors) (**G**). **H**, **I** Percentages of TOX^{+}TIM3^{+}/LAG3^{+} cells (**H**), and EOMES^{+}TIM3^{+}/LAG3^{+} cells (**I**) in Vδ2 T cells after co-culturing with HeLa-luci (BTN3A1-WT and BTN3A1-KO) tumor cell lines at a 1:1 ratio for 24 h ($n=3$ healthy donors). **J** An animal experimental system for in vivo evaluation of the effect of BTN3A1 on the functionality of Vδ2 T cells. **K**, **L** Percentages of IFN-γ^{+}, TNF-α^{+}, TOX^{+} and EOMES^{+} cells in Vδ2 TILs on day 8 (D20) after adoptive transfer ($n=4$ mice per group). Error bars represent mean ± SD. *p* values were calculated using two-tailed Student's *t* test. ****$p<0.0001$, ***$p<0.001$, **$p<0.01$, *$p<0.05$. ns, not significant

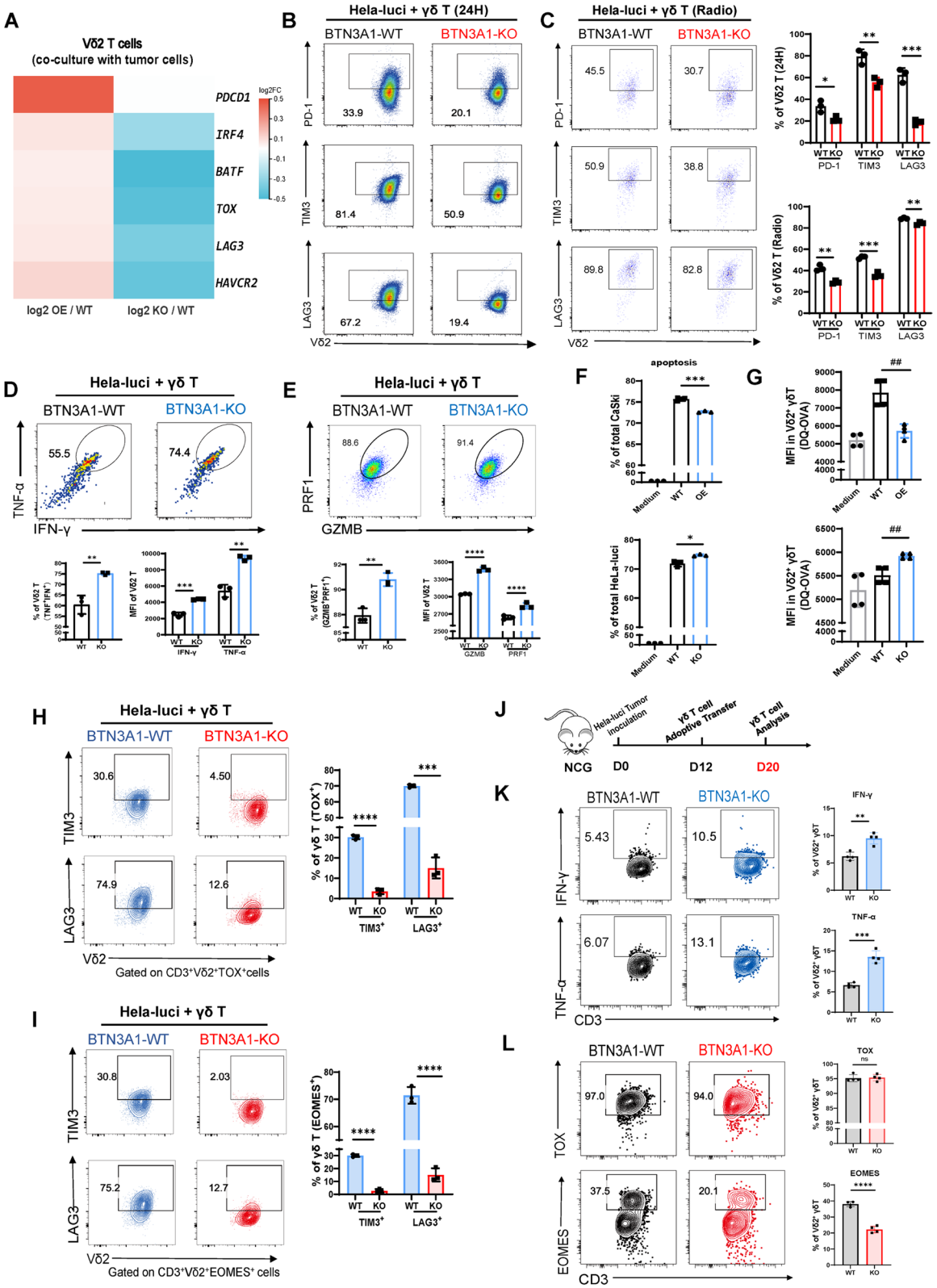

Fig. 3 (See legend on previous page.)

reported that TOX is highly expressed in exhausted T cell (T_{EX}), and EOMES, a key TF regulating T cells function, is highly expressed not only in terminally differentiated effect memory T cells (T_{EMRA}), but also in T_{EX} [24]. γδ T cells with higher levels of EOMES exhibit an exhausted phenotype and have a poorer ability to produce IFN-γ [25]. Therefore, these findings suggest the involvement of EOMES in γδ T cell exhaustion. We found that the expression of TOX and EOMES was positively correlated in CC (Figure S5A), and both were positively correlated with the expression of exhaustion-related molecules (Figure S5B). Furthermore, after co-culturing with CC cells, the frequencies of $TIM3^+TOX^+$ and $LAG3^+TOX^+$ Vδ2 T cells as well as the frequencies of $EOMES^+$, $EOMES^+TIM3^+$, $EOMES^+LAG3^+$ Vδ2 T cells were significantly increased in the BTN3A1-WT group compared to those in the BTN3A1-KO group, with further increased in the BTN3A1-OE group (Fig. 3H-I and Figure S5C-G). These results indicate that both TOX and EOMES are involved in BTN3A1-induced Vδ2 T cell exhaustion.

To validate BTN3A1-induced Vδ2 T cell exhaustion in vivo, HeLa-luci cell line was implanted subcutaneously into NCG mice, which were subsequently injected with amplified Vδ2 T cells via tail vein upon tumor grew to be palpable. After 8 days of adoptive cell transfer, the subcutaneous tumor was removed to analyze the functional molecules of Vδ2 T cells in the tumor (Fig. 3J). Obtained results were consistent with those in vitro (Fig. 3K and K). Thus, our findings collectively demonstrate that BTN3A1 can promote Vδ2 T cell exhaustion in CC.

TFs NR4A2/3 are critical in mediating BTN3A1-induced expression of exhaustion-related molecules in Vδ2 T cells

In order to explore potential factors mediating BTN3A1-induced Vδ2 T cell exhaustion, differential TFs of Vδ2 T cells in the BTN3A1-KO and BTN3A1-WT groups were enriched through RNA-seq. The NR4A family, which is part of the zf-C4 self-build, were significantly enriched in the BTN3A1-WT group (Fig. 4A). NR4As and TOX can work together to promote the exhaustion of $CD8^+$ T cells [26], and we reasoned that NR4As may also affect the exhaustion and anti-tumor capacity of Vδ2 T cells. Analysis of the TIMER 2.0 database showed that the expression levels of NR4A2 and NR4A3 (rather than NR4A1), along with γδ T cells infiltration influence the prognosis of CC patients. With the extension of follow-up time, the lower the expression levels of NR4A2/3, and the higher the infiltration level of γδ T cells, the better the prognosis of CC patients (Fig. 4B, C and Figure S6A). Next, by comparing NR4A2/3 expression in Vδ2 T cells from peripheral blood and tumor tissue of CC patients, it was found that both the frequency and the expression levels of $NR4A2^+$ and $NR4A3^+$ Vδ2 T cells were higher in tumor tissue than in peripheral blood (Fig. 4D). Moreover, in the peripheral blood and tumor tissue of CC patients, the expression levels of NR4A2/3 in $PD\text{-}1^+$ Vδ2 T cells were consistently higher than those in $PD\text{-}1^-$ Vδ2 T cells (Figure S6B). Therefore, NR4A2/3 TFs are significantly correlated with Vδ2 T cells exhaustion.

To investigate the regulatory effect of BTN3A1 on NR4A2/3 of Vδ2 T cells, CC cell lines with different expression levels of BTN3A1 were co-cultured with Vδ2 T cells for 24 and 48 h, respectively. Compared with those in the BTN3A1-WT group, the expressions of NR4A2/3 in Vδ2 T cells of the BTN3A1-KO group were lower, while showed an increasing trend in the BTN3A1-OE group (Fig. 4E and Figure S6C). Moreover, the proportion of $NR4A2^+$ or $NR4A3^+$ Vδ2 T cells co-expressed with PD-1, TIM3, and LAG3 were all significantly lower in the BTN3A1-KO group, while showed an increasing trend in the BTN3A1-OE group compared to those in the BTN3A1-WT group (Fig. 4F, Figure S7A-C). Importantly, knockdown NR4A2 or NR4A3 by transfection of siRNA into Vδ2 T cells both resulted in significantly downregulated PD-1, TIM3, and LAG3 in Vδ2 T cells co-cultured with BTN3A1-sufficient HeLa-luci cells (the BTN3A1-WT group) (Fig. 4G). Interestingly, NR4A2 knockdown in Vδ2 T cells significantly downregulated the expressions of TOX and EOMES, while NR4A3 knockdown downregulated their expressions to

(See figure on next page.)

Fig. 4 BTN3A1 regulates NR4A2/3 TFs of Vδ2 T cells. **A** Dot plot showing differential transcription factors of Vδ2 T cells co-cultured with HeLa-luci (BTN3A1-KO *vs.* BTN3A1-WT) tumor cell lines at a 1:1 ratio for 24 h ($n = 2$ replicates per group). **B**, **C** The correlation between the combination of mRNA expression levels of *NR4A2* (**B**), *NR4A3* (**C**) and infiltration level of γδ T cells, and the cumulative survival rate of CC patients in the TCGA database ($n = 306$). **D** Percentages of $NR4A2^+$ and $NR4A3^+$ cells, and MFIs of NR4A2 and NR4A3 in Vδ2 T cells from peripheral blood ($n = 20$) and tumor tissue ($n = 13$) of CC patients. **E** Percentages of $NR4A2^+$ and $NR4A3^+$ cells in Vδ2 T cells after co-culturing Vδ2 T cells with HeLa-luci (BTN3A1-WT and BTN3A1-KO) or CaSki (BTN3A1-WT and BTN3A1-OE) tumor cell lines at a 1:1 ratio for 24 h ($n = 3$ healthy donors). **F** Percentages of $NR4A2/3^+PD\text{-}1^+$, $NR4A2/3^+TIM3^+$ and $NR4A2/3^+LAG3^+$ cells in Vδ2 T cells after co-culturing Vδ2 T cells with HeLa-luci (BTN3A1-WT and BTN3A1-KO) tumor cell lines at a 1:1 ratio for 24 h ($n = 3$ healthy donors). **G** Percentages of $PD\text{-}1^+$, $TIM3^+$ and $LAG3^+$ cells in Vδ2 T cells transfected with siNR4A2/3 after co-culturing Vδ2 T cells with HeLa-luci (BTN3A1-WT and BTN3A1-KO) tumor cell lines at a 1:1 ratio for 24 h ($n = 3$ replicates per group). Error bars represent mean ± SD. *p* values were calculated using two-tailed Student's *t* test. ****/####$p < 0.0001$, ***$p < 0.001$, **$p < 0.01$, *$p < 0.05$. ns, not significant

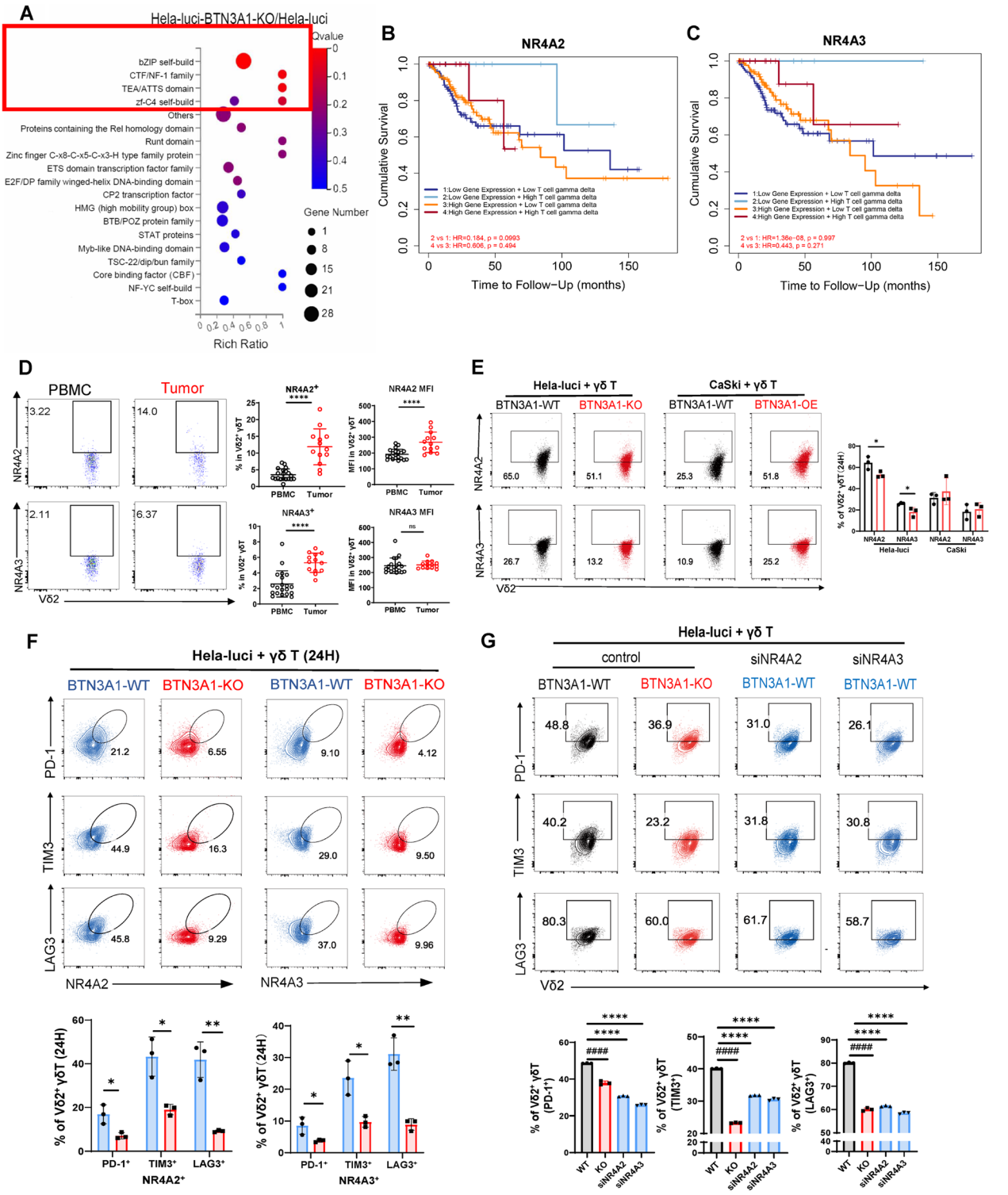

Fig. 4 (See legend on previous page.)

a less extent (Figure S7D). Therefore, BTN3A1 regulates the expression of exhausted molecules and related TFs in Vδ2 T cells through NR4A2/3.

γδ TCR is required for BTN3A1-induced Vδ2 T cell exhaustion

Through KEGG enrichment analysis of differentially expressed genes in Vδ2 T cells co-cultured with

HeLa-luci cell lines (BTN3A1-KO and BTN3A1-WT) for 24 h revealed that the top two ranked pathways were TCR and NF-κB signaling pathways (Fig. 5A). Key molecules participating in the TCR signaling pathway in Vδ2 T cells of the BTN3A1-KO group were lower than those of the BTN3A1-WT group, supporting the hypothesis that the TCR signaling pathway was less stimulated without BTN3A1. Meanwhile, compared to the BTN3A1-WT group, the expression levels of representative molecules in the NF-κB signaling pathway in Vδ2 T cells of the BTN3A1-KO group were lower, while the expression level of IKBα that decomposes P65 was higher (Fig. 5B). These results together indicate the important role of BTN3A1 in stimulating the TCR and NF-κB signaling pathways in Vδ2 T cells.

Vδ2 T cells co-cultured with BTN3A1-sufficient CC cells show stronger TCR signaling compared to those co-cultured with BTN3A1-deficient CC cells. We hypothesized that strong TCR engagement by BTN3A1 induces Vδ2 T cell exhaustion. To test this hypothesis, Vγ9 blocking antibody was added to the co-culture system, which significantly downregulated the expression levels of PD-1, TIM3, and LAG3 in Vδ2 T cells of the BTN3A1-WT group (Fig. 5C and D), as well as the proportion of $NR4A2^+$ or $NR4A3^+$ Vδ2 T cells co-expressing these markers (Fig. 5E and Figure S8A), indicating the necessity of the BTN3A1-TCR interaction. To evaluate the role of NF-κB signaling pathway in mediating Vδ2 T cell exhaustion, Vδ2 T cells were pretreated with the NF-κB signaling pathway inhibitor JSH-23. The results showed that JSH-23 did not show a uniform trend in the expression of PD-1, TIM3, and LAG3. However, it led to reduce expression of TFs TOX and EOMES in Vδ2 T cells in both groups, and the differential expression of EOMES between the two groups was eliminated (Fig. 5F).

γδ T cells not only recognize phosphorylated antigens/BTN3A1 through γδ TCRs, but are also capable of sensing stress-related ligands through NKG2D receptors [27]. To exclude the confounding effect of NKG2D on evaluating the role of BTN3A1 in inducing Vδ2 T cell exhaustion, we compared the frequencies of $PD\text{-}1^+$, $TIM3^+$, and $LAG3^+$ cells in both $NKG2D^+$ and $NKG2D^-$ Vδ2 T cells compartment between the BTN3A1-WT and BTN3A1-KO groups, and did not find any differences (Figure S8B). At the same time, it was found that NKG2D ligands (ULBP1/2 and MICA/B) do not correlate with BTN3A1 in the TME (Figure S8C). Therefore, BTN3A1 directly interacts with Vγ9 receptor to regulate downstream NR4A2/3 and influence exhausted molecules, while also affecting the NF-κB signaling pathway to regulate TOX and EOMES.

BTN3A1 upregulates PD-L1 expression in tumor cells by promoting IFN-γ secretion in Vδ2 T cells

We have shown that BTN3A1 on tumor cells can promote the expression of PD-1 on Vδ2 T cells. In triple negative breast cancer patients, high expression of PD-L1 can keep Vδ2 T cells in an exhausted state [28], and in pancreatic cancer, PD-L1 binds with PD-1 to promote Vδ2 T cell exhaustion [29]. Therefore, the PD-1/PD-L1 interactions may enhance the effect of BTN3A1 on Vδ2 T cell exhaustion. Analysis of TCGA database revealed a positive correlation between the expression of BTN3A1 and PD-L1 in CC (Fig. 6A). Interestingly, BTN3A1 did not affect the expression of PD-L1 in tumor cells when cultured alone (Fig. 6B), indicating that the TME may play a crucial role in this process. Co-culturing CC cells with Vδ2 T cells revealed that high PD-L1 expression in both tumor cells and Vδ2 T cells when tumor cells with higher expression of BTN3A1 (Fig. 6C, D, Figure S9A and S9B).

Numerous studies have shown that IFN-γ can induce the expression of PD-L1 in tumor cells [30, 31]. Therefore, the IFN-γ secreted by Vδ2 T cells activated during co-culture with CC cells may promote the expression of PD-L1 on tumor cells. We first detected IFN-γ secreted into the supernatant. As expected, Vδ2 T cells accumulated more IFN-γ when co-cultured with BTN3A1-WT tumor cells than when co-cultured with BTN3A1-KO tumor cells (Fig. 6E). It should be noted that this experiment, which detects the secretion of IFN-γ into the supernatant during the whole co-culture stage, is different from those presented in the previous study, which measured the potential of Vδ2 T cells to produce IFN-γ

(See figure on next page.)

Fig. 5 BTN3A1 regulates TCR signaling pathway. **A**, **B** Bar chart showing $\log_{10}$FC fold changes for the differentially expressed genes of KEGG pathway after co-culturing Vδ2 T cells with HeLa-luci (BTN3A1-WT and BTN3A1-KO) tumor cell lines at a 1:1 ratio for 24 h, the purified Vδ2 T cells were subjected to RNA-seq ($n=2$ replicates per group) (**A**); the expression levels of key molecules in the TOP2 pathway (TCR signaling pathway and NF-κB signaling pathway) of co-cultured Vδ2 T cells were verified (**B**). **C**-**E** Percentages of $PD\text{-}1^+$, $TIM3^+$, and $LAG3^+$ cells in Vδ2 T cells (**C**, **D**), and percentages of $NR4A2^+PD\text{-}1^+$, $NR4A2^+TIM3^+$ and $NR4A2^+LAG3^+$ cells in Vδ2 T cells (**E**), after co-culturing with HeLa-luci (BTN3A1-WT and BTN3A1-KO) tumor cell lines at a 1:1 ratio for 24 h in the presence or absence of Vγ9 neutralizing antibodies ($n=3$ healthy donors). **F** Percentages of TOX^+ and $EOMES^+$ cells in Vδ2 T cells after pretreating Vδ2 T cells with NF-κB signaling pathway inhibitors JSH-23 (10 ng/ml) for 1 h and then co-culture with HeLa-luci (BTN3A1-WT and BTN3A1-KO) tumor cell lines at a 1:1 ratio for 24 h ($n=4$ healthy donors). Error bars represent mean ± SD. *p* values were calculated using two-tailed Student's *t* test. ****/####$p<0.0001$, ***$p<0.001$, **/##$p<0.01$, */#$p<0.05$. ns, not significant

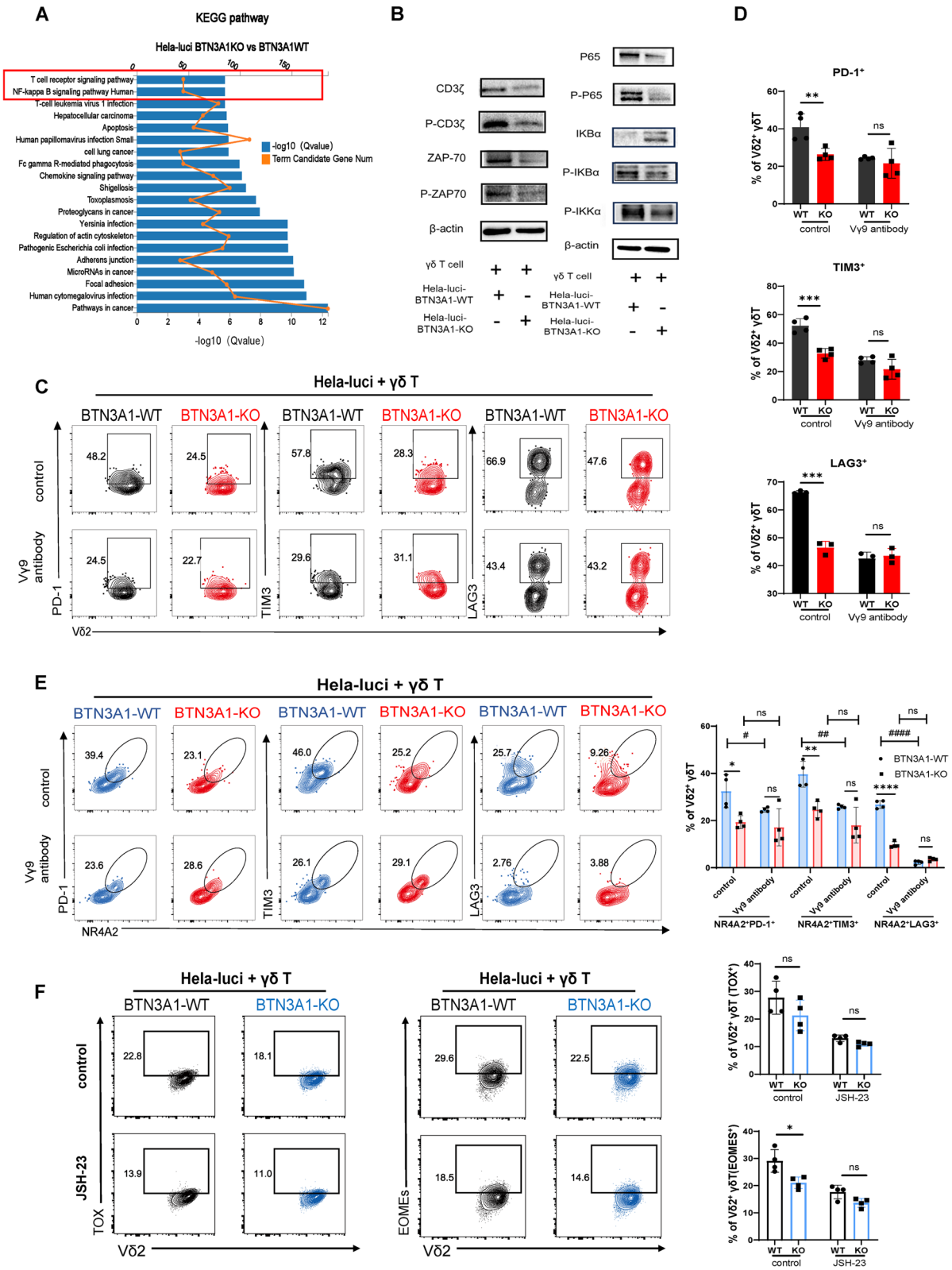

Fig. 5 (See legend on previous page.)

at the end of co-culture. Meanwhile, adding anti-IFN-γ neutralizing antibody significantly downregulated PD-L1 expression in both tumor cells and Vδ2 T cells (Fig. 6F), suggesting that BTN3A1 can promote the expression of PD-L1 in the TME through inducing Vδ2 T cells to secrete IFN-γ. Furthermore, through analyzing data extracted from public database, we found that high expression of BTN3A1 in tumor was correlated with a better response rate to anti-PD-1/PD-L1 antibody treatment (Fig. 6G) and a higher survival rate in patients (Fig. 6H).

Previous studies have shown that IFN-γ can induce the expression of BTN3A1 on monocytes. Therefore, we speculated that similar to the regulation of PD-L1 expression, the expression of BTN3A1 in CC cells might also be upregulated by IFN-γ. To test this, we stimulated CC cells with IFN-γ and found that IFN-γ can significantly increase the expression of BTN3A1 in tumor cells (Figure S9C). Similarly, in the co-culture system, both CC cells and Vδ2 T cells increased their expression of BTN3A1 (Fig. 6I and Figure S9D), which can be partially counteracted by anti-IFN-γ neutralizing antibodies (Fig. 6I). Taken together, these findings suggest that BTN3A1 expressed by CC cells indirectly promotes the expressions of BTN3A1 and PD-L1 through inducing Vδ2 T cells to secrete IFN-γ, thereby constituting a feedforward loop that accelerates the exhaustion program.

Discussion

Immunotherapy with checkpoint blockade has shown some benefit for CC patients, especially when combined with other therapies, but overall efficacy is still not satisfactory [32]. These may be partially attributable to the functional impairment of αβ T cells and the presence of immunosuppressive tumor-associated macrophages in the TME of CC [33, 34]. γδ T cell–based immunotherapy is a promising option therapeutic for CC treatment, as the presence of γδ tumor-infiltrating lymphocytes (TILs) are associated with a better prognosis. Even without checkpoint inhibitors, adoptive transfer of Vδ2 T cells expanded in vitro has shown anti-tumor effects [35], indicating their potential clinical application. However, unlike $CD8^+$ T cells, the anti-tumor response of Vδ2 T cells does not improve with higher cell numbers [36], suggesting that γδ T cells may experience exhaustion in the TME, limiting their ability to control tumor growth.

We found that prolonged BTN3A1-TCR engagement results in Vδ2 T cell exhaustion instead of activation through inducing profound changes of TFs including TOX, EOMES, and NR4A. It has been reported that the downstream signal transduction cascades downstream of TCR engagement are extremely complicated, with many signaling pathways involved and interconnected. For example, TCR engagement activates the PKCθ and MAPK/ERk pathways, both of which can promote TF NF-κB activity. At the same time, it also can trigger the calcium signaling pathway and further affect the expression of related TFs [37]. This complexity is also exemplified by our findings that the BTN3A1-TCR interaction can affect TOX and EOMES either through NR4A2/3 downstream of TCR engagement, or via NF-κB signaling pathway in Vδ2 T cells. However, whether the cross-regulation of NR4A2/3 and NF-κB signaling pathways exists is still an open question. Therefore, further research is needed to confirm the detailed regulatory pathways involved and whether the exhaustion regulatory network in $CD8^+$ T cells is also applicable to Vδ2 T cells.

It has been well-established that continuous TCR stimulation of $CD8^+$ T cells in chronic infection and TME can lead to their functional exhaustion [13]. However, recent studies have shown that $CD8^+$ T cells can downregulate their function and express exhaustion-related molecules within as rapidly as 12 h of contacting with tumor cells [38]. Our research indicated that BTN3A1 expressed on tumor cells can indeed increase the expression of exhaustion-related inhibitory molecules and TFs in Vδ2 T cells amplified in vitro through γδ TCR receptors within 24 h,

(See figure on next page.)

Fig. 6 IFN-γ secreted by Vδ2 T cells promotes the expression of BTN3A1 and PD-L1. **A** The correlation between *BTN3A1* and *CD274* mRNA expression levels in CC patients in the TCGA database ($n = 306$). **B** The expression level of PD-L1 in HeLa-luci (BTN3A1-WT and BTN3A1-KO) and CaSki (BTN3A1-WT and BTN3A1-OE) tumor cell lines. **C**, **D** The percentage of $PD\text{-}L1^+$ cells in tumor cells **C** and Vδ2 T cells **D** after co-culturing HeLa-luci (BTN3A1-WT and BTN3A1-KO) tumor cell lines with Vδ2 T cells at a 1:1 ratio for 24 or 48 h ($n = 3$ healthy donors). **E** The concentration of IFN-γ in supernatant after co-culture HeLa-luci (BTN3A1-WT and BTN3A1-KO) tumor cell lines with Vδ2 T cells at a 1:1 ratio for 6 h ($n = 4$ healthy donors) and 24 h ($n = 3$ healthy donors). **F** MFI of PD-L1 in tumor cells and Vδ2 T cells after co-culturing HeLa-luci (BTN3A1-WT and BTN3A1-KO) tumor cell lines with Vδ2 T cells at a 1:1 ratio for 24 h in the presence or absence of anti-IFN-γ (10 ng/ml) ($n = 5$ healthy donors). **G** The correlation between mRNA expression level of *BTN3A1* and patient survival rate in tumor patients receiving anti-PD-1/PD-L1 treatment. **H** The correlation between *BTN3A1* mRNA expression level and tumor patient response to anti-PD-1/PD-L1 treatment. **I** MFI of BTN3A1 in tumor cells and Vδ2 T cells after co-culturing HeLa-luci (BTN3A1-WT and BTN3A1-KO) tumor cell lines with Vδ2 T cells at a 1:1 ratio for 24 h in the presence or absence of anti-IFN-γ (10 ng/ml) ($n = 4$ healthy donors). Error bars represent mean ± SD. *p* values were calculated using two-tailed Student's *t* test. $^{****}p < 0.0001$, $^{***}p < 0.001$, $^{**}p < 0.01$, $^{*}p < 0.05$. ns, not significant

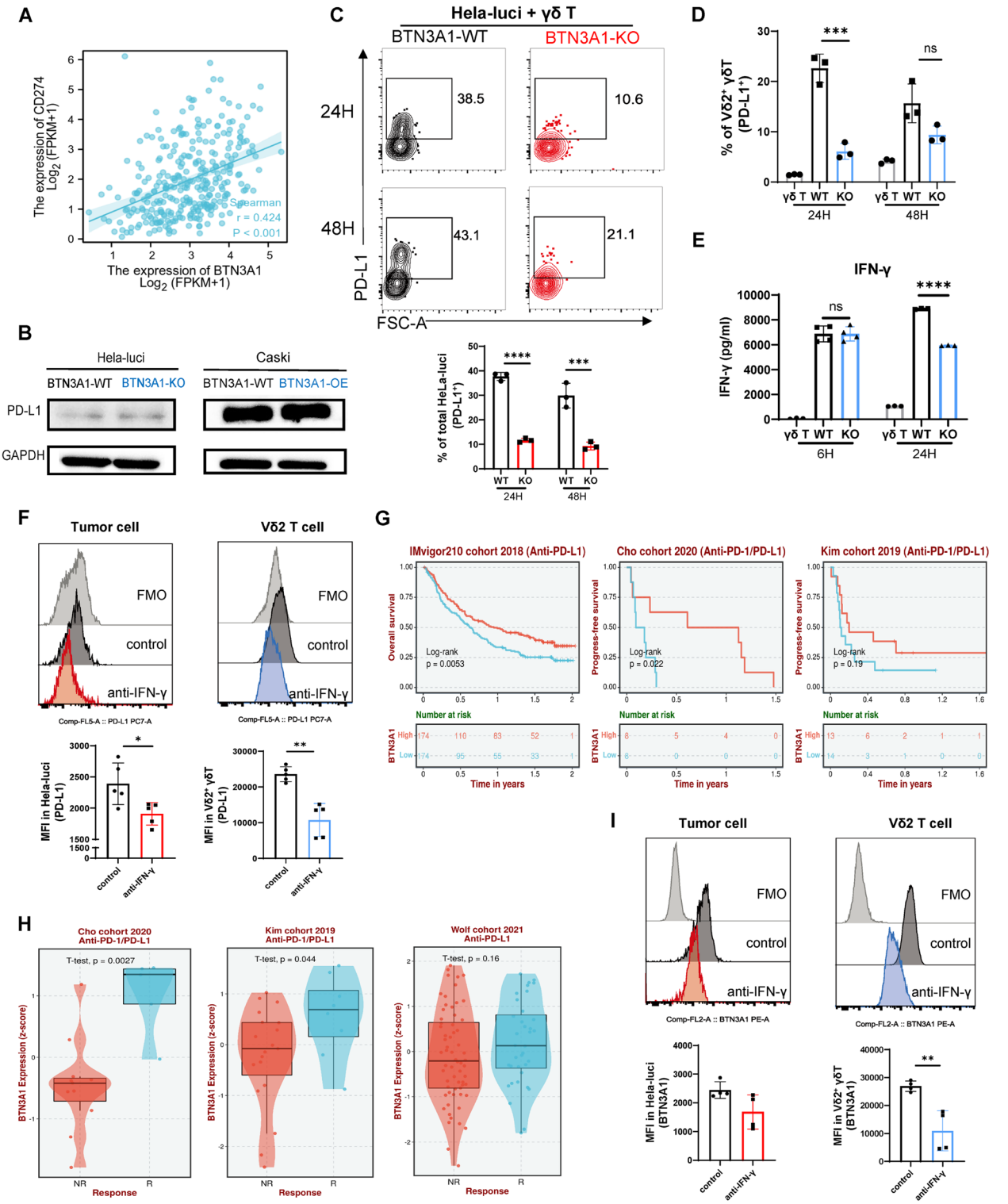

Fig. 6 (See legend on previous page.)

albeit Vδ2 T cells still retain strong anti-tumor ability. Therefore, further exploration is needed to determine the extent to which BTN3A1 expressed by tumor cells affects Vδ2 T cells functional exhaustion. In addition, whether it is sustained or reversible is also worth further interrogation.

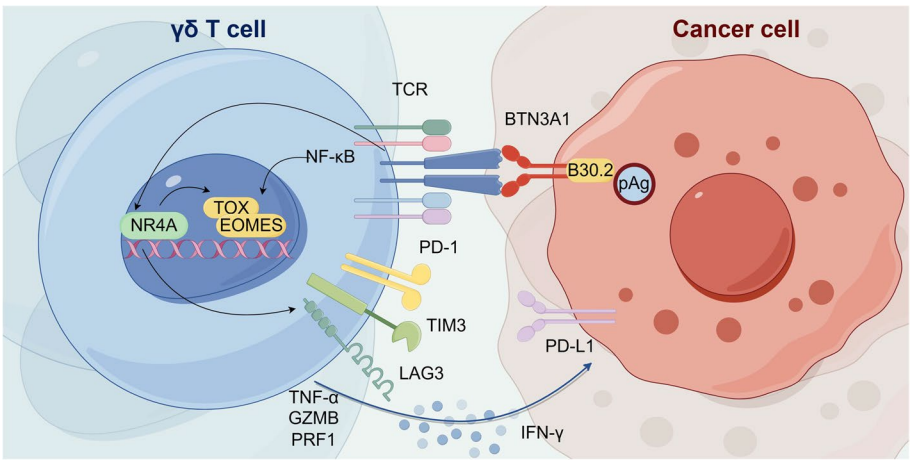

Fig. 7 BTN3A1 expressed on CC tumor cells induces exhaustion of γδ T cells through γδ TCR signaling pathway. (By Figdraw). Upon extended engagement of TCR with BTN3A1 expressed by cancer cells, Vδ2 T cells upregulate the expression of NR4A2/3 and NF-κB, which in turn increase the expression of TFs TOX and EOMES, leading to the elevated expression of exhausted molecules (PD-1, TIM3, LAG3). IFN-γ produced by Vδ2 T cells after their extended interaction with BTN3A1-expressing CC cells is still capable of inducing the expression of BTN3A1 and PD-L1 in CC cells, thereby further promoting the exhaustion of Vδ2 T cells

BTN3A1 is widely expressed on an array of cell types, including immune cells and tumor cells [39, 40]. In addition to the impact of BTN3A1 expressed by tumor cells on Vδ2 T cells as revealed in this study, BTN3A1 expressed in antigen-presenting cells is pivotal in pAg-induced Vδ2 T cell activation [41], which is actually the basis of most in vitro protocols for Vδ2 T cell expansion. In addition, BTN3A1 also regulates the immune activity of $CD4^+$ T, $CD8^+$ T, monocytes, and NK cells, thereby playing a more extensive role in regulating the immune system [39]. With regard to its role in regulating Vδ2 T cells, the expression levels of BTN3A1 in different cells may have different effects on Vδ2 T cells. However, given the lack of Vδ2 T cell counterpart in mice, and the differences of BTN3A1 across species, it is difficult to construct a suitable tumor model to further explore the relationship between them in vivo. Nevertheless, further interrogation of the impact of BTN3A1 on different immune cells could have a profound impact on future combinatorial immunotherapy.

BTN3A1 has been found to be highly expressed in pancreatic cancer, rectal cancer [42, 43] and ovarian cancer [44], which is consistent with our observations in CC and suggests the pro-tumoral role of BTN3A1. In the PD-L1 humanized system, targeting BTN3A1 can overcome the highly immunosuppressive microenvironment of ovarian cancer and is more effective than neutralizing PD-L1/PD-1 checkpoints in delaying malignant progression [44]. The regulatory mechanism of BTN3A1 expression in CC cells is still unclear, and studies have reported that both IFN-γ and TNF-α can promote the expression of BTN in endothelial cells [45]. IFN-γ can also promote Vδ2 T cells activation by inducing the expression of BTN3A1 in monocytes [46]. Here, Vδ2 T cells infiltration and the expression level of IFN-γ in CC tissue positively correlated with BTN3A1 expression, and this correlation was consistent with that between PD-L1 and IFN-γ. Furthermore, our study demonstrated that Vδ2 T cells activated by BTN3A1 secreted IFN-γ, which in turn induced the expression of PD-L1 and BTN3A1 in CC cells, thereby further aggravating the immunosuppressive microenvironment. Therefore, the expression pattern and regulatory mechanism of BTN3A1 is highly similar to PD-L1, suggesting that BTN3A1 may be another novel immune checkpoint molecule in CC. Therefore, combining immune checkpoint therapy with γδ T cell–based immunotherapy may achieve twice the result with half the effort.

Conclusion

In summary, our findings indicate that expanded Vδ2 T cells contact with BTN3A1 of tumor cells through γδ TCR receptor, and this interaction leads to the upregulation of exhausted molecules and further downregulation of their function (Fig. 7). BTN3A1 affects TFs TOX and EOMES through TFs NR4A2/3 downstream of TCR signaling pathway, or through NF-κB signaling pathway, thereby regulating the expression of exhaustion-related molecules (PD-1, TIM3 and LAG3) in Vδ2

T cells. Moreover, despite the functional impairment of Vδ2 T cells following sustained interaction with BTN3A1-expressing CC cells, they still retain the ability to produce IFN-γ, which induces the expression of BTN3A1 and PD-L1 in CC cells, further promoting the exhaustion of Vδ2 T cells. Our study provides insights into the mechanism behind γδ T cells exhaustion in the TME and lays the groundwork for future clinical translation of γδ T cell-based immunotherapy.

Abbreviations

APC	Antigen presentation cell
CC	Cervical cancer
CDX	Cell line-derived xenograft
CTV	Cell Trace violet
DFS	Disease-free survival
ELISA	Enzyme linked immunosorbent assay
GZMB	Granzyme B
ICIs	Immune checkpoint inhibitors
KO	Knockout
MHC	Major histocompatibility complex
NFAT	Nuclear factor of activated T cells
NR4A	Nuclear receptor subfamily 4 group A
OE	Overexpression
OS	Overall survival
pAg	Phosphorantigen
PBMC	Peripheral blood mononuclear cell
PFS	Progression-free survival
PRF1	Perforin
TCGA	The Cancer Genome Atlas
T_{EMRA}	Terminally differentiated effect memory T cell
T_{EX}	Exhausted T cell
TF	Transcription factor
TILs	Tumor-infiltrating lymphocytes
TME	Tumor microenvironment

Supplementary Information

The online version contains supplementary material available at https://doi.org/10.1186/s12964-024-01834-0.

Supplementary Material 1.

Supplementary Material 2. Supplemental figure 1. (A) Proportion of Vδ2 T cells in all living cells and the MFI of Vδ2 during the expansion of Vδ2 T cells (Day 0, Day 4, Day 8, Day 12, Day 16, and Day 20) using PBMCs from healthy individuals ($n = 3$ healthy donors). (B, C) KEGG analysis (B) and GO analysis (C) of differentially expressed genes in the high and low expression groups of BTN3A1 in the GSEA dataset (GSE44001) ($n = 300$). (D) The correlation between the mRNA expression level of *BTN3A1* and disease-free survival (DFS) in CC patients in the GSEA dataset (GSE44001) ($n = 300$, left) and in the TCGA dataset ($n = 170$, right). (E) The correlation between the abundance of γδ T cells in CC patients and their cumulative survival rate in the TCGA database ($n = 306$). Error bars represent mean ± SD. *p* values were calculated using two-tailed Student's*t* test. ****$p< 0.0001$, ***$p< 0.001$, **$p< 0.01$, *$p< 0.05$. ns, not significant.GSEA, Gene Set Enrichment Analysis. Supplemental figure 2. (A) MFI of BTN3A1 in CC cell lines (CaSki, C33A, SiHa-luci, ME180, MS751 and HeLa-luci) ($n = 3$ replicates per group). (B) Detecting proliferation of HeLa-luci (BTN3A1-WT and BTN3A1-KO) tumor cell lines culturing at day 0, day 1, day 2, and day 3 through CCK-8. (C) The relative mRNA expression levels of HPV-E6 and HPV-E7 in CC cell lines (CaSki, C33A, SiHa and HeLa) ($n = 4$ replicates per group). (D) Validation of the constructed cell lines (C33A-Vector and C33A-E7-OE) with E7 overexpression (left), and detection of the relative mRNA expression level of *BTN3A1* in CC cell lines (right) ($n = 5$ replicates per group). (E) Percentage of IL-17A$^+$ cells in Vδ2 T cells after co-culturing C33A (E7-Vector and E7-OE) tumor cell lines with expanded Vδ2 T cells at a 1:1 ratio or PBMC at a 10:1 ratio for 6 hours (n = 3 healthy donors). Error bars represent mean ± SD. *p* values were calculated using two-tailed Student's *t* test. ****$p< 0.0001$, ***$p< 0.001$, **$p< 0.01$, *$p< 0.05$. ns, not significant. Supplemental figure 3 (A, B) Percentages of PD-1$^+$, TIM3$^+$, and LAG3$^+$ cells in Vδ2 T cells after co-culturing with HeLa-luci (BTN3A1-WT and BTN3A1-KO) tumor cell lines at a 1:1 ratio for 48 hours (A), or with CaSki (BTN3A1-WT and BTN3A1-OE) tumor cell lines at a 1:1 ratio for 24 or 48 hours (B) ($n = 3$ healthy donors). (C) Percentages of PD-1$^+$TIM3$^+$ cells in Vδ2 T cells after co-culturing Vδ2 T cells with HeLa-luci (BTN3A1-WT and BTN3A1-KO) tumor cell lines, or with CaSki (BTN3A1-WT, BTN3A1-OE) tumor cell lines at a 1:1 ratio for 24 ($n = 3$ healthy donors). (D, E) Percentage of IFN-γ$^+$TNF-α$^+$ cells and MFIs of IFN-γ and TNF-α in Vδ2 T cells after co-culturing with HeLa-luci (BTN3A1-WT and BTN3A1-KO) tumor cell lines at a 1:1 ratio for 48 hours (D), or with CaSki (BTN3A1-WT, BTN3A1-OE) tumor cell lines at a 1:1 ratio for 24 or 48 hours (E) ($n = 3$ healthy donors). (F, G) Dilution of CTV after Vδ2 T cells co-culturing with HeLa-luci (BTN3A1-WT and BTN3A1-KO) tumor cell lines at a 1:1 ratio for 24 or 48 hours (F), or with CaSki (BTN3A1-WT and BTN3A1-OE) tumor cell lines at a 1:1 ratio for 72 or 96 hours (G) ($n = 3$ healthy donors). Error bars represent mean ± SD. *p* values were calculated using two-tailed Student's*t* test. ****$p< 0.0001$, ***$p< 0.001$, **$p< 0.01$, *$p< 0.05$. ns, not significant. Supplemental figure 4. (A, B) Percentages of HLADR$^+$ and CD86$^+$ cells in Vδ2 T cells after co-culturing Vδ2 T cells with HeLa-luci (BTN3A1-WT and BTN3A1-KO) tumor cell lines at a 1:1 ratio for 24 or 48 hours (A), or with CaSki (BTN3A1-WT, BTN3A1-OE) tumor cell lines at a 1:1 ratio for 24 or 48 hours (B) ($n = 3$ replicates per group). Error bars represent mean ± SD. *p* values were calculated using two-tailed Student's *t* test. **$p< 0.01$, *$p< 0.05$. ns, not significant. Supplemental figure 5 (A, B) The correlation between *TOX* and *EOMES* mRNA expression levels (A), and the correlation between *TOX* or *EOMES* and *PDCD1*, *HAVCR2*, *LAG3* (B) in CC patients in the TCGA database ($n = 306$). (C, D) Percentages of TOX$^+$TIM3$^+$ and TOX$^+$LAG3$^+$ cells (C) in Vδ2 T cells after co-culturing with HeLa-luci (BTN3A1-WT and BTN3A1-KO) tumor cell lines for 48 hours; CaSki (BTN3A1-WT and BTN3A1-OE) tumor cell lines for 24 or 48 hours at a 1:1 ratio (n= 3 healthy donors) (D). (E-G) Percentages of EOMES$^+$ cells (E), EOMES$^+$TIM3$^+$ and EOMES$^+$LAG3$^+$ cells in Vδ2 T cells after co-culturing with HeLa-luci (BTN3A1-WT and BTN3A1-KO) tumor cell lines for 48 hours (F) and CaSki (BTN3A1-WT and BTN3A1-OE) tumor cell lines for 24 or 48 hours (G) at a 1:1 ratio ($n = 3$ healthy donors). Error bars represent mean ± SD. *p* values were calculated using two-tailed Student's*t* test. ***$p< 0.001$, **$p< 0.01$, *$p< 0.05$. ns, not significant. Supplemental figure 6. (A) The correlation between the combination of the mRNA expression level of *NR4A1* and the infiltration level of γδ T cells, and the cumulative survival rate of CC patients in the TCGA database ($n = 306$), analyzed using TIMER 2.0. (B) MFI of NR4A2 and NR4A3 in PD-1$^+$ and PD-1$^-$ Vδ2 T cells from peripheral blood ($n = 20$) and tumor tissue ($n = 13$) of CC patients. (C) Percentages of NR4A2$^+$, NR4A3$^+$cells in Vδ2 T cells after co-culturing Vδ2 T cells with HeLa-luci (BTN3A1-WT and BTN3A1-KO) or CaSki (BTN3A1-WT and BTN3A1-OE) tumor cell lines at a 1:1 ratio for 48 hours ($n = 3$ healthy donors). Error bars represent mean ± SD. *p* values were calculated using two-tailed Student'sttest. ****$p< 0.0001$, ***$p< 0.001$, **$p< 0.01$, *$p< 0.05$. ns, not significant. Supplemental figure 7. (A-C) Percentages of NR4A2/3$^+$PD-1$^+$, NR4A2/3$^+$TIM3$^+$and NR4A2/3$^+$LAG3$^+$ cells in Vδ2 T cells after co-culturing Vδ2 T cells with HeLa-luci (BTN3A1-WT and BTN3A1-KO) tumor cell lines at a 1:1 ratio for 48 hours (A) or with CaSki (BTN3A1-WT and BTN3A1-OE) tumor cell lines at a 1:1 ratio for 24 hours (B) or 48 hours (C) ($n = 3$ healthy donors). (D) Percentages of TOX$^+$ and EOMES$^+$ cells in Vδ2 T cells transfected with siNR4A2 or siNR4A3 after co-culturing Vδ2 T cells with HeLa-luci (BTN3A1-WT and BTN3A1-KO) tumor cell lines at a 1:1 ratio for 24 hours ($n = 3$ replicates per group). Error bars represent mean ± SD. *p* values were calculated using two-tailed Student'sttest. ****/####$p< 0.0001$, ***$p< 0.001$, **$p< 0.01$, *$p< 0.05$. ns, not significant. Supplemental figure 8. (A) Percentages of NR4A3$^+$PD-1$^+$, NR4A3$^+$TIM3$^+$ and NR4A3$^+$LAG3$^+$ cells in Vδ2 T cells after co-culturing Vδ2 T cells with HeLa-luci (BTN3A1-WT and BTN3A1-KO) tumor cell lines at a 1:1 ratio for 24 hours in the presence or absence of Vγ9 neutralizing antibodies ($n = 3$ healthy donors). (B) Percentages of PD-1$^+$, TIM3$^+$, and LAG3$^+$ cells in NKG2D$^+$ or NKG2D$^-$ Vδ2 T cells after co-culturing Vδ2 T cells with HeLa-luci (BTN3A1-WT and BTN3A1-KO) tumor cell lines at a 1:1 ratio for 24 hours ($n = 3$ healthy donors). (C) Correlations between *BTN3A1* and *ULBP1/2,*

MICA/B in CC patients in the TCGA database ($n = 306$). Error bars represent mean ± SD. *p* values were calculated using two-tailed Student's*t* test. ****$p< 0.0001$, **$p< 0.01$, *$p< 0.05$. ns, not significant. Supplemental figure 9. (A, B) The percentage of PD-L1$^+$ cells in tumor cells (A) and Vδ2 T cells (B) after Vδ2 T cells co-culturing with CaSki (BTN3A1-WT and BTN3A1-OE) tumor cell lines at a 1:1 ratio for 24 or 48 hours ($n = 3$ healthy donors). (C) Percentage of BTN3A1$^+$ cells in HeLa and CaSki tumor cell lines for 24 hours in the presence or absence of IFN-γ (100 ng/ml) stimulation ($n = 3$ healthy donors). (D) MFI of BTN3A1 in Vδ2 T cells of PBMC before expansion (Day 0), after expansion (Day 12), and after co-culturing with HeLa-luci (BTN3A1-WT and BTN3A1-KO) tumor cell lines ($n = 3$ healthy donors) following expansion. Error bars represent mean ± SD. *p* values were calculated using two-tailed Student's *t* test. ****$p< 0.0001$, ***$p< 0.001$, **$p< 0.01$, *$p< 0.05$.

Acknowledgements
We thank all the patients and healthy donors who participated in this study.

Authors' contributions
Jian Liu drafted, conceptualized the manuscript; Jian Liu Min Wu, Hui Wang, Yafei Huang and Xun Tian conceived the idea, designed the experiments; Jian Liu and Min Wu conducted all the experiments; Yifan Yang, Xinyu Mei, Liming Wang, Jingyu Wang, Zixuan Wang, Shan He, Hangyu Liu, Han Jiang, Shen Qu, Yuwei Zhang, Ying Chen contributed to specific sections and revised the manuscript; Hui Wang, Yafei Huang, Xun Tian provided overall supervision for the manuscript and revised the manuscript. All authors read and approved the final manuscript.

Funding
This study was supported by the National Key Research and Development Program of China (No.2021YFC2701204 to H.W.), the National Natural Science Foundation of China (No.82373260 to H.W.), the "Jianbing" and "Lingyan" R&D programs of Zhejiang province (No.2022C03013 to H.W.), the National Natural Science Foundation of China (82172584). (4 + X) Preliminary study on the efficacy and safety of tumor infiltrating lymphocyte (TIL) in the treatment of refractory recurrent/advanced gynecological tumors (LY2022004 to H.W.).

Availability of data and materials
The datasets used and/or analyzed during the current study are available from the corresponding author on reasonable request.

Data availability
Data is provided within the manuscript or supplementary information files.

Declarations

Ethics approval and consent to participate
This study was approved by the Medical Ethics Committee of Tongji Medical College, Huazhong University of Science and Technology (Approval No. [2021] S034). Written informed consents were obtained from all participants before study entry.

Consent for publication
Not applicable.

Competing interests
The authors declare no competing interests.

Author details
[1]Department of Obstetrics and Gynecology, Tongji Hospital, Tongji Medical College, Huazhong University of Science and Technology, Wuhan, China. [2]School of Basic Medicine, Tongji Medical College, Huazhong University of Science and Technology, Wuhan, China. [3]Department of Gynecologic Oncology, Women's Hospital, Zhejiang University School of Medicine, Hangzhou, Zhejiang, China. [4]Department of Obstetrics and Gynecology, Academician Expert Workstation, The Central Hospital of Wuhan, Tongji Medical College, Huazhong University of Science and Technology, Wuhan, Hubei 430014, China. [5]Department of Pathogen Biology, School of Basic Medicine, Tongji Medical College, Huazhong University of Science and Technology, Wuhan, China. [6]State Key Laboratory for Diagnosis and Treatment of Severe Zoonotic Infectious Diseases, Huazhong University of Science and Technology, Wuhan, China. [7]Cancer Biology Research Center (Key Laboratory of the Ministry of Education), Tongji Hospital, Tongji Medical College, Huazhong University of Science and Technology, Wuhan, China. [8]Zhejiang Key Laboratory of Precision Diagnosis and Therapy for Major Gynecological Diseases, Women's Hospital, Zhejiang University School of Medicine, Hangzhou, Zhejiang, China.

Received: 3 June 2024 Accepted: 17 September 2024
Published online: 28 September 2024

References

1. Singh D, Vignat J, Lorenzoni V, Eslahi M, Ginsburg O, Lauby-Secretan B, et al. Global estimates of incidence and mortality of cervical cancer in 2020: a baseline analysis of the WHO Global Cervical Cancer Elimination Initiative. Lancet Glob Health. 2023;11(2):e197–206. https://doi.org/10.1016/S2214-109X(22)00501-0.
2. Cohen PA, Jhingran A, Oaknin A, Denny L. Cervical cancer. The Lancet. 2019;393(10167):169–82. https://doi.org/10.1016/s0140-6736(18)32470-x.
3. Liu L, Li S, Wang G, Qu Y, Wang Z, Duan J, et al. Dynamic toxicity landscape of immunotherapy for solid tumors across treatment lines. J Natl Cancer Cent. 2023;3(3):186–96. https://doi.org/10.1016/j.jncc.2023.07.002.
4. Silva-Santos B, Mensurado S, Coffelt SB. gammadelta T cells: pleiotropic immune effectors with therapeutic potential in cancer. Nat Rev Cancer. 2019;19(7):392–404. https://doi.org/10.1038/s41568-019-0153-5.
5. Kabelitz D, Serrano R, Kouakanou L, Peters C, Kalyan S. Cancer immunotherapy with gammadelta T cells: many paths ahead of us. Cell Mol Immunol. 2020;17(9):925–39. https://doi.org/10.1038/s41423-020-0504-x.
6. Sebestyen Z, Prinz I, Dechanet-Merville J, Silva-Santos B, Kuball J. Translating gammadelta (gammadelta) T cells and their receptors into cancer cell therapies. Nat Rev Drug Discov. 2020;19(3):169–84. https://doi.org/10.1038/s41573-019-0038-z.
7. Wilhelm M, Kunzmann V, Eckstein S, Reimer P, Weissinger F, Ruediger T, et al. Gammadelta T cells for immune therapy of patients with lymphoid malignancies. Blood. 2003;102(1):200–6. https://doi.org/10.1182/blood-2002-12-3665.
8. Yi Y, He HW, Wang JX, Cai XY, Li YW, Zhou J, et al. The functional impairment of HCC-infiltrating gammadelta T cells, partially mediated by regulatory T cells in a TGFbeta- and IL-10-dependent manner. J Hepatol. 2013;58(5):977–83. https://doi.org/10.1016/j.jhep.2012.12.015.
9. Castella B, Foglietta M, Riganti C, Massaia M. Vgamma9Vdelta2 T Cells in the Bone Marrow of Myeloma Patients: A Paradigm of Microenvironment-Induced Immune Suppression. Front Immunol. 2018;9:1492. https://doi.org/10.3389/fimmu.2018.01492.
10. Zakeri N, Hall A, Swadling L, Pallett LJ, Schmidt NM, Diniz MO, et al. Characterisation and induction of tissue-resident gamma delta T-cells to target hepatocellular carcinoma. Nat Commun. 2022;13(1):1372. https://doi.org/10.1038/s41467-022-29012-1.
11. Chen D, Guo Y, Jiang J, Wu P, Zhang T, Wei Q, et al. gammadelta T cell exhaustion: Opportunities for intervention. J Leukoc Biol. 2022;112(6):1669–76. https://doi.org/10.1002/JLB.5MR0722-777R.
12. Wherry EJ, Kurachi M. Molecular and cellular insights into T cell exhaustion. Nat Rev Immunol. 2015;15(8):486–99. https://doi.org/10.1038/nri3862.
13. Seo W, Jerin C, Nishikawa H. Transcriptional regulatory network for the establishment of CD8(+) T cell exhaustion. Exp Mol Med. 2021;53(2):202–9. https://doi.org/10.1038/s12276-021-00568-0.
14. Liu X, Wang Y, Lu H, Li J, Yan X, Xiao M, et al. Genome-wide analysis identifies NR4A1 as a key mediator of T cell dysfunction. Nature. 2019;567(7749):525–9. https://doi.org/10.1038/s41586-019-0979-8.
15. Pauken KE, Sammons MA, Odorizzi PM, Manne S, Godec J, Khan O, et al. Epigenetic stability of exhausted T cells limits durability of reinvigoration by PD-1 blockade. Science. 2016;354(6316):1160–5. https://doi.org/10.1126/science.aaf2807.
16. Vavassori S, Kumar A, Wan GS, Ramanjaneyulu GS, Cavallari M, El Daker S, et al. Butyrophilin 3A1 binds phosphorylated antigens and stimulates human gammadelta T cells. Nat Immunol. 2013;14(9):908–16. https://doi.org/10.1038/ni.2665.

17. Gu SY, Sachleben JR, Boughter CT, Nawrocka WI, Borowska MT, Tarrasch JT, et al. Phosphoantigen-induced conformational change of butyrophilin 3A1 (BTN3A1) and its implication on Vγ9Vδ2 T cell activation. P Natl Acad Sci USA. 2017;114(35):E7311–20. https://doi.org/10.1073/pnas.1707547114.
18. Liang F, Zhang C, Guo H, Gao SH, Yang FY, Zhou GB, et al. Comprehensive analysis of BTN3A1 in cancers: mining of omics data and validation in patient samples and cellular models. FEBS Open Bio. 2021;11(9):2586–99. https://doi.org/10.1002/2211-5463.13256.
19. Rigau M, Uldrich AP, Behren A. Targeting butyrophilins for cancer immunotherapy. Trends Immunol. 2021;42(8):670–80. https://doi.org/10.1016/j.it.2021.06.002.
20. Arnett HA, Viney JL. Immune modulation by butyrophilins. Nat Rev Immunol. 2014;14(8):559–69. https://doi.org/10.1038/nri3715.
21. Gao Z, Bai Y, Lin A, Jiang A, Zhou C, Cheng Q, et al. Gamma delta T-cell-based immune checkpoint therapy: attractive candidate for antitumor treatment. Mol Cancer. 2023;22(1):31. https://doi.org/10.1186/s12943-023-01722-0.
22. Rancan C, Arias-Badia M, Dogra P, Chen B, Aran D, Yang H, et al. Exhausted intratumoral Vdelta2(-) gammadelta T cells in human kidney cancer retain effector function. Nat Immunol. 2023;24(4):612–24. https://doi.org/10.1038/s41590-023-01448-7.
23. Blank CU, Haining WN, Held W, Hogan PG, Kallies A, Lugli E, et al. Defining "T cell exhaustion." Nat Rev Immunol. 2019;19(11):665–74. https://doi.org/10.1038/s41577-019-0221-9.
24. Zhang L, Yu X, Zheng L, Zhang Y, Li Y, Fang Q, et al. Lineage tracking reveals dynamic relationships of T cells in colorectal cancer. Nature. 2018;564(7735):268–72. https://doi.org/10.1038/s41586-018-0694-x.
25. Lino CNR, Barros-Martins J, Oberdörfer L, Walzer T, Prinz I. Eomes expression reports the progressive differentiation of IFN-γ-producing Th1-like γδ T cells. Eur J Immunol. 2017;47(6):970–81. https://doi.org/10.1002/eji.201646753.
26. Seo H, Chen J, Gonzalez-Avalos E, Samaniego-Castruita D, Das A, Wang YH, et al. TOX and TOX2 transcription factors cooperate with NR4A transcription factors to impose CD8(+) T cell exhaustion. Proc Natl Acad Sci U S A. 2019;116(25):12410–5. https://doi.org/10.1073/pnas.1905675116.
27. Dokouhaki P, Schuh NW, Joe B, Allen CA, Der SD, Tsao MS, et al. NKG2D regulates production of soluble TRAIL by ex vivo expanded human gammadelta T cells. Eur J Immunol. 2013;43(12):3175–82. https://doi.org/10.1002/eji.201243150.
28. Li P, Wu R, Li K, Yuan W, Zeng C, Zhang Y, et al. IDO Inhibition Facilitates Antitumor Immunity of Vgamma9Vdelta2 T Cells in Triple-Negative Breast Cancer. Front Oncol. 2021;11(2234–943x):679517. https://doi.org/10.3389/fonc.2021.679517.
29. Daley D, Zambirinis CP, Seifert L, Akkad N, Mohan N, Werba G, et al. gammadelta T Cells Support Pancreatic Oncogenesis by Restraining alphabeta T Cell Activation. Cell. 2016;166(6):1485–99 e15. https://doi.org/10.1016/j.cell.2016.07.046.
30. Ivashkiv LB. IFNgamma: signalling, epigenetics and roles in immunity, metabolism, disease and cancer immunotherapy. Nat Rev Immunol. 2018;18(9):545–58. https://doi.org/10.1038/s41577-018-0029-z.
31. Schroder K, Hertzog PJ, Ravasi T, Hume DA. Interferon-gamma: an overview of signals, mechanisms and functions. J Leukoc Biol. 2004;75(2):163–89. https://doi.org/10.1189/jlb.0603252.
32. Monk BJ, Enomoto T, Kast WM, McCormack M, Tan DSP, Wu X, et al. Integration of immunotherapy into treatment of cervical cancer: Recent data and ongoing trials. Cancer Treat Rev. 2022;106:102385. https://doi.org/10.1016/j.ctrv.2022.102385.
33. Zheng Y, Wang Y, Zou C, Hu B, Zhao M, Wu X. Tumor-Associated Macrophages Facilitate the Proliferation and Migration of Cervical Cancer Cells. Oncologie. 2022;24(1):147–61. https://doi.org/10.32604/oncologie.2022.019236.
34. Wang Y, Fan P, Feng Y, Yao X, Peng Y, Wang R. Clinical implication of naive and memory T cells in locally advanced cervical cancer: A proxy for tumor biology and short-term response prediction. Biocell. 2023;47(6):1365–75. https://doi.org/10.32604/biocell.2023.027201.
35. Zumwalde NA, Sharma A, Xu XQ, Ma SD, Schneider CL, Romero-Masters JC, et al. Adoptively transferred Vγ9Vδ2 T cells show potent antitumor effects in a preclinical B cell lymphomagenesis model. Jci Insight. 2017;2(13):e93179. https://doi.org/10.1172/jci.insight.93179.
36. Nada MH, Wang H, Hussein AJ, Tanaka Y, Morita CT. PD-1 checkpoint blockade enhances adoptive immunotherapy by human Vgamma-2Vdelta2 T cells against human prostate cancer. Oncoimmunology. 2021;10(1):1989789. https://doi.org/10.1080/2162402X.2021.1989789.
37. Burbach BJ, Medeiros RB, Mueller KL, Shimizu Y. T-cell receptor signaling to integrins. Immunol Rev. 2007;218(0105–2896 (Print)):65–81.https://doi.org/10.1111/j.1600-065X.2007.00527.x.
38. Rudloff MW, Zumbo P, Favret NR, Roetman JJ, Detres Roman CR, Erwin MM, et al. Hallmarks of CD8(+) T cell dysfunction are established within hours of tumor antigen encounter before cell division. Nat Immunol. 2023;24(9):1527–39. https://doi.org/10.1038/s41590-023-01578-y.
39. Kone AS, Ait Ssi S, Sahraoui S, Badou A. BTN3A: A Promising Immune Checkpoint for Cancer Prognosis and Treatment. Int J Mol Sci. 2022;23(21).https://doi.org/10.3390/ijms232113424.
40. Chen S, Li Z, Huang W, Wang Y, Fan S. Prognostic and Therapeutic Significance of BTN3A Proteins in Tumors. J Cancer. 2021;12(15):4505–12. https://doi.org/10.7150/jca.57831.
41. Yuan L, Ma X, Yang Y, Qu Y, Li X, Zhu X, et al. Phosphoantigens glue butyrophilin 3A1 and 2A1 to activate Vγ9Vδ2 T cells. Nature. 2023;621(7980):840–8. https://doi.org/10.1038/s41586-023-06525-3.
42. Benyamine A, Loncle C, Foucher E, Blazquez J-L, Castanier C, Chrétien A-S, et al. BTN3A is a prognosis marker and a promising target for Vγ9Vδ2 T cells based-immunotherapy in pancreatic ductal adenocarcinoma (PDAC). OncoImmunology. 2018;7(1):e1372080. https://doi.org/10.1080/2162402X.2017.1372080.
43. Zocchi MR, Costa D, Venè RA-O, Tosetti F, Ferrari N, Minghelli S, et al. Zoledronate can induce colorectal cancer microenvironment expressing BTN3A1 to stimulate effector γδ T cells with antitumor activity. Oncoimmunology. 2017;6(3):e1278099. https://doi.org/10.1080/2162402X.2016.1278099.
44. Payne KK, Mine JA, Biswas S, Chaurio RA, Perales-Puchalt A, Anadon CM, et al. BTN3A1 governs antitumor responses by coordinating alphabeta and gammadelta T cells. Science. 2020;369(6506):942–9. https://doi.org/10.1126/science.aay2767.
45. Compte E, Pontarotti P, Collette Y, Lopez M, Olive D. Frontline: Characterization of BT3 molecules belonging to the B7 family expressed on immune cells. Eur J Immunol. 2004;34(8):2089–99. https://doi.org/10.1002/eji.200425227.
46. Zhou JQ, Zhang JJ, Tao L, Peng KX, Zhang QA, Yan KX, et al. Up-regulation of BTN3A1 on CD14+ cells promotes Vγ9Vδ2 T cell activation in psoriasis. Proc Natl Acad Sci USA. 2022;119(44):e2117523119. https://doi.org/10.1073/pnas.2117523119.

Publisher's Note